Published in final edited form as:
J Med Chem. 2018 May 10; 61(9): 4067–4086. doi:10.1021/acs.jmedchem.8b00091.

Strategic Approaches to Overcome Resistance against Gram-Negative Pathogens Using β-Lactamase Inhibitors and β-Lactam Enhancers: Activity of Three Novel Diazabicyclooctanes WCK 5153, Zidebactam (WCK 5107), and WCK 4234

Krisztina M. Papp-Wallace[*,†,‡,§], **Nhu Q. Nguyen**[§], **Michael R. Jacobs**[‡,#], **Christopher R. Bethel**[†], **Melissa D. Barnes**[†,‡], **Vijay Kumar**[§], **Saralee Bajaksouzian**[‡,#], **Susan D. Rudin**[†,‡], **Philip N. Rather**[¶,○], **Satish Bhavsar**[∇], **Tadiparthi Ravikumar**[∇], **Prasad K. Deshpande**[∇], **Vijay Patil**[∇], **Ravindra Yeole**[∇], **Sachin S. Bhagwat**[∇], **Mahesh V. Patel**[∇], **Focco van den Akker**[*,§], and **Robert A. Bonomo**[*,†,‡,§,‖,⊥]

[†]Research Service, Louis Stokes Cleveland Department of Veterans Affairs Medical Center, 10701 East Boulevard, Cleveland, Ohio 44106, United States

[‡]Department of Medicine, Case Western Reserve University School of Medicine, Cleveland, Ohio 44106, United States

[§]Department of Biochemistry, Case Western Reserve University School of Medicine, Cleveland, Ohio 44106, United States

[‖]Department of Pharmacology, Case Western Reserve University School of Medicine, Cleveland, Ohio 44106, United States

[⊥]Department of Molecular Biology and Microbiology, Case Western Reserve University School of Medicine, Cleveland, Ohio 44106, United States

[#]Department of Pathology, University Hospitals, Cleveland Medical Center, Cleveland, Ohio 44106, United States

[*]**Corresponding Authors**: Phone: 216-791-3800 ×6230. Krisztina.Papp@va.gov. Phone: 216-368-8511. fxv5@case.edu. Phone: 216-791-3800 × 4801. Robert.Bonomo@va.gov.

Author Contributions

K.M.P.W, M.R.J, S.S.B, M.V.P, F.v.d.A., and R.A.B. designed the project. K.M.P.W., N.Q.N, C.R.B., M.D.B, V.K., S.B., S.D.R., S.B., T.R., P.K.D., V.P., and R.Y. performed experiments. P.N.R provided critical reagents. K.M.P.W, M.R.J, S.S.B, M.V.P, F.v.d.A., and R.A.B. analyzed the results together and wrote the manuscript. All authors read and approved the manuscript.

ASSOCIATED CONTENT

Supporting Information

Tables S1–S2, Figure S1, and SMILES. The Supporting Information is available free of charge on the ACS Publications website at DOI: 10.1021/acs.jmedchem.8b00091.

Electron density of compounds **1–3** bound in the active site of KPC-2 obtained by cocrystallization experiments, data collection and refinement statistics for KPC-2 and OXA-24/40 bound to compounds **1–3**, MICs for laboratory-engineered *A. baumannii* knockout strains (PDF)

SMILES (CSV)

Accession Codes

KPC-2-soaked **1** (PDB ID: 6B1X), KPC-2-soaked **2** (PDB ID: 6B1J), KPC-2-soaked **3** (PDB ID: 6B1F), KPC-2-cocrystallized **1** (PDB ID: 6B1Y), KPC-2-cocrystallized **2** (PDB ID: 6B1W), KPC-2-cocrystallized **3** (PDB ID: 6B1H), OXA-24/40-cocrystallized **3** (PDB ID: 6B22).

The authors declare the following competing financial interest(s): S.B., T.R., P.K.D., V.P., R.Y., S.S.B., and M.V.P. are employees of Wockhardt Research Centre, Aurangabad, India.

[¶]Department of Microbiology and Immunology, Emory University School of Medicine Atlanta, Georgia 30322, United States

[○]Research Service, Atlanta VA Medical Center, Decatur, Georgia 30033, United States

[▽]Wockhardt Research Centre, Aurangabad, India

Abstract

Limited treatment options exist to combat infections caused by multidrug-resistant (MDR) Gram-negative bacteria possessing broad-spectrum β-lactamases. The design of novel β-lactamase inhibitors is of paramount importance. Here, three novel diazabicyclooctanes (DBOs), WCK 5153, zidebactam (WCK 5107), and WCK 4234 (compounds 1–3, respectively), were synthesized and biochemically characterized against clinically important bacteria. Compound 3 inhibited class A, C, and D β-lactamases with unprecedented k_2/K values against OXA carbapenemases. Compounds 1 and 2 acylated class A and C β-lactamses rapidly but not the tested OXAs. Compounds 1–3 formed highly stable acyl-complexes as demonstrated by mass spectrometry. Crystallography revealed that 1–3 complexed with KPC-2 adopted a “chair conformation” with the sulfate occupying the carboxylate binding region. The cefepime-2 and meropenem-3 combinations were effective in murine peritonitis and neutropenic lung infection models caused by MDR *Acinetobacter baumannii*. Compounds 1–3 are novel β-lactamase inhibitors that demonstate potent cross-class inhibition, and clinical studies targeting MDR infections are warranted.

Abstract

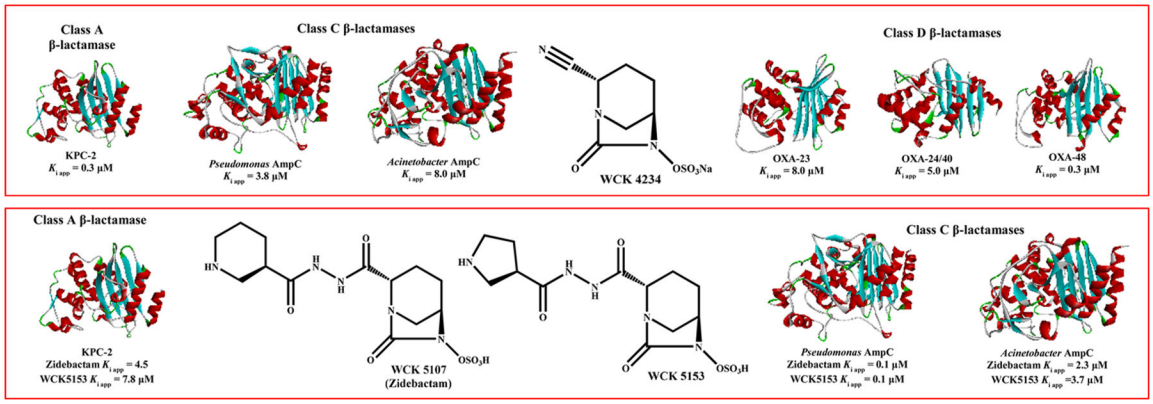

INTRODUCTION

In February of 2017, carbapenem-resistant Enterobacteriaceae (CRE), *Pseudomonas aeruginosa*, and *Acinetobacter baumannii* were designated as the “top priority pathogens” for the development of novel antibiotics by the World Health Organization.[1] The presence of β-lactamases in these Gram-negative pathogens is largely responsible for this global threat. Of the serine β-lactamases, *Klebsiella pneumoniae* carbapenemase (KPC), *Pseudomonas*-derived cephalosporinase (PDC), *Acinetobacter*-derived cephalosporinase (ADC), and the carbapenem-hydrolyzing class D OXA β-lactamases (e.g., OXA-23, OXA-24/40, and OXA-48) represent the most prevalent and problematic β-lactam inactivating hydrolases.

Presently, three strategies are used by the pharmaceutical industry to overcome β-lactamase-mediated resistance: (i) the design of new β-lactams resistant to hydrolysis, (ii) the synthesis of new β-lactamase inhibitors (BLIs), and (iii) the development of new antimicrobial classes.[2] An emerging and appealing strategy to overcome diverse mechanisms of β-lactamase-mediated resistance deploys an unconventional concept of a β-lactam enhancer (BLE). BLEs represent a new antimicrobial class and work by providing complementary penicillin binding protein (PBP) inhibition to a partner β-lactam. By targeting two different PBPs, BLEs act synergistically to promote killing of the bacterial cell. Thus, a remarkable aspect of the BLE mechanism is that it can operate independently of BLIs.

The BLIs currently available in the clinic in the United States are clavulanic acid (approved in 1984), sulbactam (approved in 1986), tazobactam (approved in 1993), avibactam (approved in 2015), and vaborbactam (approved in 2017). During the past 30 years, clavulanic acid, sulbactam, and tazobactam have lost efficacy against inhibitor-resistant TEMs (IRTs) and inhibitor-resistant SHVs (IRSs).[2] With the exception of tazobactam demonstrating fair activity as an inhibitor against certain class C cephalosporinases (CMY-2, K_i = 40 μM),[3] these three BLIs possess poor or no activity against the recently emerged class A carbapenemases (e.g., KPC), class B metallo-β-lactamases (e.g., NDM and VIM), and many class D OXA β-lactamases.

Diazabicyclooctanes (DBOs) are a new class of BLIs (“second generation” BLIs) that were developed in the early 2000s.[2] Avibactam, the first DBO introduced into clinical practice, inhibits class A carbapenemases, KPC, as well as class C β-lactamases, AmpCs, and when combined with ceftazidime has the ability to target many drug-resistant Enterobacteriaceae.[2,4–8] Avibactam, however, possesses limited activity toward class D OXA β-lactamases.[4,9] Avibactam is slow to acylate OXA-type β-lactamases with low k_2/K values in the range of 10^1-10^3 M^{-1} s^{-1}. In contrast, avibactam acylates class A and class C β-lactamases in the range of 10^3–10^6 M^{-1} s^{-1}. The recently described atomic structures of OXA-24/40 and OXA-48 revealed that the binding pocket, especially where the R^1 side chain of avibactam resides in class D β-lactamases, is more hydrophobic with fewer polar residues present, thus potentially affecting binding and acylation of avibactam.[7,8]

In the past decade, the DBO class of BLIs expanded to include novel DBOs with modified chemical scaffolds that enhance their activity. The first generation DBO inhibitors avibactam and relebactam inactivate class A, C, and some class D β-lactamases.[4,10] The DBO inhibitors WCK 5153 (compound **1**), zidebactam, formerly WCK 5107 (compound **2**), nacubactam, FPI-1465, and ETX2514 are “dual action inhibitors” as they inhibit PBPs and certain β-lactamases as well as possess BLE activity.[8,11–13] Compounds **1** and **2** were shown to be potent inactivators of *P. aeruginosa* PBP-2 and *A. baumannii* PBP-2 resulting in enhanced killing of bacteria when combined with a β-lactam partner.[11]

Two challenges need to be overcome to design BLIs with promising therapeutic potential against class D OXA β-lactamases associated with *Acinetobacter* spp. The first is to readily access the sterically constrained active site of such β-lactamases found in the periplasm and imparting inhibitory activity. The second is to effectively traverse the outer membrane and periplasmic space embedded with diverse efflux pumps. Newer generations of BLIs such as

avibactam, relebactam, and vaborbactam are devoid of activity against class D OXA β-lactamases, which illustrates the challenge in designing such compounds. Sulbactam, which is an "older" or legacy BLI, effectively permeates the outer membrane and reaches the periplasmic compartment of *Acinetobacter*. However, sulbactam fails to inhibit class D OXA β-lactamases, additional evidence of formidable scientific intricacy of the field. This challenge led us to explore the effects of introduction of a nitrile functional group onto the DBO core. Unlike avibactam and relebactam, WCK 4234 (compound **3**), possessing a nitrile side chain (R^1) at the C2 position of the DBO (Figure 1), demonstrates expanded activity against class D OXA β-lactamases, including OXA-23 and OXA-51 expressed in *A. baumannii*, while maintaining activity against class A and C β-lactamases.[14]

The structure—activity relationships (SAR) that prompted the design of compounds **1–3** are presented herein. Furthermore, we evaluate **1–3** and two DBO comparators, avibactam and relebactam (Figure 1, chemical structures), to gain mechanistic insights into their inhibitory activity against representative serine class A, C, and D β-lactamases using steady-state kinetics and mass spectrometry. As a result of these studies, KPC-2 and OXA-24 were chosen for X-ray crystallography analysis to define, on an atomic level, the nature of the inactivation mechanism. Finally, the abilities of cefepime-**2** (WCK 5222) and meropenem-**3** (WCK 5999) combinations were evaluated in susceptibility studies and mouse models of infection. Our data show that cefepime-**2** and meropenem-**3** offer promise against pathogens possessing β-lactamases from multiple classes. Notably, the cefepime-**2** combination has completed two phase I clinical trials (NCT02707107, NCT02532140), and another phase I clinical trial is actively recruiting participants (NCT02942810).

RESULTS AND DISCUSSION

Synthesis of a Novel Class of DBOs.

Starting with a DBO scaffold, a pathway to identify compounds with activity against Gram-negative PBP-2 and β-lactamases led to the evolution of this novel bicyclo hydrazide (BCH) series.[11] The key medicinal chemistry challenge involved in identifying a side chain (R^1) at the C-2 position of the DBO core that was able to penetrate the periplasmic space of Gram-negative bacteria and access PBP targets on the cytoplasmic membrane. After developing SAR with linear-chain and cyclic amines,[15] a cyclic secondary amine was employed on the acyl hydrazide to obtain compounds with high affinity binding for the PBP-2 of *Enterobacteriaceae, P. aeruginosa*, and *A. baumannii*.[11] Thus, the hydrazide as an R^1 side chain bearing a free amine at the appropriate length from the C-2 position of the DBO core was found to be essential for antibacterial potency. Enhancement of antibacterial activity was further achieved by chiral separation of the isomers of the racemic secondary cyclic amine. SAR generated the lead compounds **1**[16] and **2**[17] and bearing pyrrolidine and piperidine side chains, respectively (Figure 2A). These compounds demonstrated a targeted antibacterial profile encompassing Enterobacteriaceae and nonfermenter organisms.[11]

To obtain a DBO that demonstrates expanded antimicrobial activity against *A. baumannii* producing class D carbapenemases, OXA-23 and OXA-51, while maintaining activity in Gram negatives producing class A and C β-lactamases,[14] we next examined the properties of the nitrile group in the literature.[18] Because nitrile bonds are polarized, they act as hydrogen

acceptors and form hydrogen bonds with amino acids and water and can thus bind to a protein backbone. Furthermore, the strong dipolar nature of the nitrile permits it to act as a hydroxyl or carboxyl bioisostere. The introduction of nitrile additionally reduces the clogP of the molecule thereby reducing its lipophilicity and thus improving the chances of penetration of the porin channels in Gram-negative organisms. The nitrile group is not readily metabolized, which could be advantageous. Importantly, the nitrile reduces the steric bulk of the R^1 substituent of DBOs such as avibactam and thus could yield a better fit into sterically constrained active sites, such as the class D OXA β-lactamase's active site. On the basis of our observations, we replaced the amide functionality of avibactam with a nitrile, generating compound **3** (Figure 2B).

Compound 3 is a Highly Potent Inactivator of Class A, C, and D β-Lactamases.

Compound **3** inhibited all β-lactamases tested with $K_{i\ app}$ values ranging from 0.1 to ≤8 μM (Table 1). Testing KPC-2, 3 possessed the highest acylation rate (k_2/K value) by nearly 9-fold compared to relebactam. Additionally, **3** was the only DBO capable of acylating OXA-23, OXA-24/40, and OXA-48. The highest k_2/K value obtained was with OXA-48 and **3**, $6.4 \pm 0.6 \times 10^5\ M^{-1}\ s^{-1}$.

The rate (k_{off}) at which the DBOs deacylate (recyclize) the β-lactamases to reform active DBO was also determined (Table 1). The rank order of 3's recyclization after inhibition was as follows: PDC-3 ≫ ADC-7 > OXA-48 > OXA-23 > OXA-24/40 > KPC-2. After inhibition by **3**, PDC-3 recovered the ability to hydrolyze nitrocefin the fastest.

The k_{off} values correspond to the residence time half-lives as listed in Table 1. Comparing all of the k_{off} values, avibactam was the DBO with the lowest k_{off} values. The β-lactamases/DBO combination with the longest residence time half-life was OXA-24/40 and avibactam at 1,823 min.[19] The turnover number (k_{cat}/kinact = t_n) at 24 h or the number of inhibitor molecules hydrolyzed before the β-lactamase is inactivated was also measured (Table 1). KPC-2 possessed a k_{cat}/k_{inact} value of 1 for all the DBOs tested. In contrast, ADC-7 demonstrated turnover of all of the DBOs; $t_n = 6$ at 24 h. Although insignificant in terms of the bacterial cell cycle, the basis for this catalytic ability is being investigated. For the relative t_n values to be put into context, the t_n of KPC-2 for clavulanic acid is 2,500 at 15 min with KPC-2 being resistant to inhibition by clavulanic acid.[20]

Compounds 1 and 2 are Potent Inhibitors of Representative AmpC β-Lactamases.

Compounds **1** and **2** possessed 3–8-fold and 18–25-fold lower $K_{i\ app}$ values against ADC-7 and PDC-3, respectively, compared to those of avibactam and relebactam (Table 1). Against ADC-7 and PDC-3, the highest acylation rates ($3.1 \pm 0.3 \times 10^4$ to $6.3 \pm 0.6 \times 10^5\ M^{-1}\ s^{-1}$) were for **1** and **2**.

Compounds 1–3 Form Highly Stable Complexes with Class A, C, and D β-Lactamases.

Upon formation of the acyl-enzyme complex between avibactam and KPC-2, avibactam was shown to desulfate (E-I*) and eventually deacylate from KPC-2 (Figure 3A and B).[4] To determine the intermediates in the reaction pathway between β-lactamase-DBO complexes

in this study, we performed timed mass spectrometry with β-lactamases that were incubated with the DBOs at an equimolar ratio for 5 min and 24 h.

The reaction intermediates between KPC-2 and either **1** (+378 ± 5 amu), **2** (+392 ± 5 amu), **3** (+247 ± 5 amu). or relebactam (+349 ± 5 amu)-formed adducts did not undergo a secondary chemical reaction; notably, desulfation was also not observed (Table 2). However, with avibactam, loss of the sulfate (–97 ± 5 amu) was demonstrated with KPC-2 after a 24 h incubation. For ADC-7, the full adducts were detected with all DBOs, except a minor loss of the sulfate (–80 ± 5 amu) was detected with **3** and avibactam at both 5 min and 24 h (Table 2). Morever, hydrolysis of **1—3** and avibactam occurred as apo-ADC-7 (40,639 ± 5 amu) was noted; only relebactam was not hydrolyzed under these conditions. These data are consistent with the k_{cat}/k_{inact} values obtained for ADC-7 at 24 h (Table 1).

During protein purification, two isoforms (40,654 ± 5 and 40,785 ± 5 amu) of the PDC-3 β-lactamase were detected. We attribute this finding to a “ragged” N-terminus (different amino acids at the N-terminus) that occurs when proteins are overexpressed. As with the ADC-7 β-lactamase, a minor loss of the sulfate side chain (–80 ± 5 amu) was observed with PDC-3 β-lactamase after incubation with **3** and avibactam at both 5 min and 24 h. When the OXA-23, OXA-24/40, or OXA-48 β-lactamases were incubated with **3**, three peaks were obtained; the major peak identified was the full adduct (+246 ± 5 amu) with two minor peaks corresponding to apoenzyme and the enzyme-DBO complex minus the sulfate (+166 ± 5 amu) at both 5 min and 24 h. In the reaction of OXA-48 β-lactamase with avibactam, only the loss of the sulfate (–80 ± 5 amu) was distinguished at 5 min. At 24 h, the full avibactam adduct (+265 ± 5 amu) was observed with the OXA-48 β-lactamase.

Interestingly, different mass adducts were discerned: a −80 amu with **3** and avibactam with the class C and D β-lactamases and −97 amu adduct with avibactam and KPC-2 (Figure 3B). Compound **3** undergoes a different desulfation mechanism (reaction) compared to the one observed with avibactam and KPC-2 as a −80 amu peak is detected corresponding to hydrolytic loss of SO_3, which is speculated to result in the hydroxylamine. The significance of this finding is being further explored.

Interactions of 1–3 with β-Lactamases are Reversible.

To confirm the reversibility of **1–3**, an acyl-transfer experiment was conducted using KPC-2 as the donor β-lactamase and TEM-1 as the recipient β-lactamase. The donor β-lactamase was preincubated with the DBO at an equimolar ratio. Then, the recipient β-lactamase was added to the reaction, and at 15 s and 5 min, the reactions were terminated and ESI-MS was conducted. Avibactam was previously shown to transfer slowly from TEM-1 to CTX-M-15 with a minor CTX-M-15-avibactam population observed at 2 min.[5] The maximum transfer of avibactam from TEM-1 to CTX-M-15 was observed at 30 min. Here, after complete inactivation (1 min incubation time) by an equimolar ratio of KPC-2 to compound **1, 2,** or **3** was obtained; then, an equimolar amount of TEM-1 was added, and the reactions were terminated by the addition of 1% acetonitrile and 0.1% formic acid. The mass spectrometry results implied that **1–3** are reversible (Figure 3C). Within 15 s, **3** transferred to TEM-1,

whereas for **1** and **2**, 5 min was required. Compounds **1—3** transfer faster than avibactam, which directly correlates to the k_{off} values observed (Table 1).

KPC-2 β-Lactamase Crystal Structures with 1–3.

The crystal structures of the DBO inhibitors **1–3** bound to KPC-2 were obtained via soaking experiments and using cocrystallization (Figure 4, Figure S1, and Table S1). The inhibitors were refined with 100% occupancy yielding low B-factors for the inhibitors (Table S1); this indicates full occupancy of the inhibitors in agreement with the appearance of strong inhibitor electron density. With each complex structure determined via these two methods, unexpected differences were obtained for the **1** and **2** structures: we observed desulfation of these two DBO inhibitors when cocrystallized but not when soaked into the KPC-2 crystals (Figure S1); these differences were not observed for **3**. Desulfation of a similar DBO, avibactam, by KPC-2 was previously also seen and found to be a slow process.[21] We subsequently probed the KPC-2-mediated desulfation of these two DBOs using mass spectrometry and also observed this phenomenon at lower pH values similar to the pH of the crystallization conditions (Figure S1). Because of the nonphysiological pH and slow rate of this reaction, our discussion will therefore focus on the structures obtained by soaking.

The three DBO inhibitors adopt a similar conformation when bound covalently to S70 in the active site of KPC-2. The 6-membered ring of the DBO adopts a chair conformation with the sulfate moiety occupying the carboxylate binding pocket of the active site. The sulfate moiety in **3** was observed to be in two conformations (Figure 4B), whereas this moiety in the other two DBOs adopted a single conformation. In all three structures, the sulfate makes hydrogen bonds with T235, T237, and S130 and is positioned ~4.5 Å from R220. The carbonyl oxygen in each of the three DBO complexes is located in the oxyanion hole formed by the backbone nitrogens of S70 and T237. The R-group moieties that distinguish the inhibitors from each other make different interactions with KPC-2. The R-group nitrile moiety in **3** makes a hydrogen bond with N132, whereas the R-groups in **1** and **2** make interactions with N132, the deacylation water (W#1), and some additional interactions with other water molecules (Figure 4B). The R-group in **2** also makes a hydrogen bond with the backbone oxygen of C238; this interaction is not observed in the avibactam:KPC-2 complex[22] nor in the relebactam:AmpC complex.[10]

The three DBO inhibitor structures are all in a very similar position and orientation as shown by superpositioning (Figure 5). These positions and orientations are very similar to that of avibactam bound to KPC-2; the ring structures of these DBOs all adopt the chair conformation (Figure 5). The KPC-2 protein in the DBO complexes also adopts a similar conformation except for residue W105 for which there is considerable conformational variability compounded by some structures even having two alternative conformations for this residue (Figure 5). We show molecule B of the **3**:KPC-2 complex in the superpositioning to further illustrate this point (Figure 5). The superpositioning also revealed a subtle clustering of the DBO ring positions with **1** and **2** in one cluster, the **3** molecule A and B in a second cluster, and avibactam in a third slightly different orientation (Figure 5). These differences are likely due to the different R-group substituents.

OXA-24/40-Compound 3 Crystal Structure.

We next analyzed a structure of 3 bound to the OXA-24/40 β-lactamase (Figure 6A and B). Overall, **3** binds to the OXA-24/40 β-lactamase in a similar fashion to that when bound to KPC-2 except for a few changes mostly due to differences between the protein. Compound **3** is covalently bound to the catalytic S81 residue. Compound **3**'s sulfate moiety interacts with R261, S219, K218, and S128. The carbonyl oxygen atom is situated in the oxyanion hole as in KPC-2. Unlike KPC-2, the nitrile moiety of **3** is not directly interacting with the protein.

In the 3-OXA-24/40 β-lactamase complex, we do not observe carboxylation of K84 as was observed in OXA-24/40 complexes bound to either penicillanic acid sulfones[23] or boronic acid inhibitors.[24] Instead, this position is filled by the presence of a chloride ion observed in two alternate positions with occupancies of 0.63 and 0.37 (labeled Cl1 and Cl2, respectively, in Figure 6C). This chloride ion is present due to the HCl used for the pH of the cacodylate buffer. Superpositioning of the **3**:OXA-24/40 structure with that of the avibactam:OXA-24/40 complex[25] indicates that avibactam and **3** have a very similar binding mode including a chair conformation of the DBO ring. The DBO inhibitors sit on the inner side of the active site bridge formed by residues M223 and Y112. The avibactam: OXA-24/40 complex has neither a carboxylated K84 nor a bound chloride ion; instead, it has CO_2 bound at this position (Figure 6C). It is interesting to note that the class D OXA β-lactamases were found to be inhibited by chloride ions that compete for the carboxylation of K84[26] including OXA-24/40;[27] the biological significance of halide binding, if any, is not yet established for OXA-24/40.

Inhibitory Activity of DBOs against Bacterial Cells.

Compound **3**, avibactam, and relebactam are BLIs. Compounds **1** and **2** can also inhibit β-lactamases but are additionally able to inactivate PBPs and serve as BLEs.[11] As a result, the DBOs either alone or in combination with either cefepime or meropenem were tested in whole cell assays to obtain minimum inhibitory concentrations (MICs). The panel of isolates selected included a set of isogenic strains expressing a single β-lactamase and clinical isolates of Enterobacteriaceae producing bla_{KPC-2} or bla_{OXA-48}, ceftazidime-avibactam-resistant *P. aeruginosa*, and *A. baumannii* producing bla_{OXA-23} and/or $bla_{OXA-24/40}$. These isolates represent some of the most difficult to treat Gram-negative pathogens, and they produce the most challenging β-lactamases to inhibit.

Isogenic *E. coli* DH10B with pBR322-*catI*-bla_{KPC-2} and *A. baumannii* Δbla_{ADC} with pWH1266 bla_{OXA-23} or bla_{OXA-24} demonstrated MICs of >16 μg/mL for cefepime and ≥8 μg/mL for meropenem (Table 3). All MICs of cefepime or meropenem combined with all five DBOs (using fixed concentrations of DBOs of 4 and/or 8 μg/mL) against *E. coli* DH10B with pBR322-*catI*-bla_{KPC-2} were reduced to ≤0.12 μg/mL. Only cefepime combined with **3** restored susceptibility for *A. baumannii* Δbla_{ADC} with pWH1266 bla_{OXA-23} (MIC = 2 μg/mL). *A. baumannii* Δbla_{ADC} with pWH1266 $bla_{OXA-24/40}$ was resistant to all combinations tested.

A panel of clinical isolates of *Klebsiella pneumoniae* that carry either bla_{KPC-2} or bla_{KPC-3} including colisitin susceptible (ColS) and colistin resistant (ColR) strains and other

Enterobacteriaceae expressing bla_{KPC} were also tested. Compounds **1–3**, avibactam, and relebactam restored susceptibility to cefepime and meropenem in all isolates (Table 3). Thus, for KPC-expressing strains, both cefepime and meropenem in combination with **3** provided comparable activity.

The DBOs were tested against a panel of clinical isolates of Enterobacteriaceae that expressed bla_{OXA-48} or bla_{OXA-48} mutants (Table 3). Compounds **1–3** and avibactam restored susceptibility to cefepime and meropenem in all isolates tested even though **1** and **2** lack inhibiton of OXA-48. Presumably, the effects of **1** and **2** are the result of PBP inhibition and their BLE property. Combinations with relebactam were less effective. Overall, Enterobacteriaceae expressing bla_{OXA-48} family members were more susceptible in combination with meropenem than with cefepime.

Five clinical strains of *P. aeruginosa* from an archived collection previously found to be resistant to ceftazidime-avibactam were also tested.[28] Combination of cefepime and **1** or **2** at 8 μg/mL restored cefepime susceptibility (MICs ≤ 0.12–0.5 μg/mL) to that of some of these highly drug resistant strains (Table 3). PBP-2 inhibition and BLE activity of **1** and **2** most likely provided this advantage against *P. aeruginosa*.[11]

The DBOs were tested against a panel of clinical isolates of *A. baumannii* that possess either bla_{OXA-23} or $bla_{OXA-24/40}$ or both bla_{OXA-23} and $bla_{OXA-24/40}$ (Table 3). Compounds **1–3** demonstrated some activity against these strains when combined with cefepime. However, against dual OXA-carbapenemase-expressing strains, most combinations showed high MICs. Given that **3** is a potent inhibitor of OXA-23 and OXA-24/40, limited penetration of cefepime and/or **3** is a possible cause of the lack of efficacy in these strains. Overall, the meropenem-**3** combination was more active against *A. baumannii* with bla_{OXA-23} and/or $bla_{OXA-24/40}$, which is in agreement with another study.[14]

For determining the cause of the higher MICs for the β-lactam-DBO combinations against *A. baumannii*, *A. baumannii* ATCC 17978 was used as the parent strain, and different efflux pump components were knocked-out as well as *blhA* (β-lactam hyper susceptibility), which is a determinant of intrinsic β-lactam resistance that is also involved in cell division. AdeABC, AdeFGH, AdeIJK, and AcrA systems are the major resistance-nodulation-division (RND) efflux systems in *Acinetobacter*. These systems are three-component efflux pumps where AdeA, AdeF, AdeI, and AcrA are the membrane fusion protein (MFP), AdeB, AdeG, and AdeJ are the multidrug transporter, and AdeC, AdeI, and AdeK are the outer membrane protein (OMP). AcrR is the transcriptional regulator of the AcrA RND efflux pump. The AdeB and AdeJ efflux pump components may have some contribution to cefepime efflux as when the corresponding genes were deleted, susceptibility was increased (Table S2). Overall, the strains were all susceptible to single agents as well as the combinations.

Cefepime-2 and Meropenem-3 Were Tested against MDR *A. baumannii* in Murine Models of Peritonitis and Neutropenic Lung Infection.

The protective doses (PD_{50} and PD_{90}, i.e., the dose of antibiotic that protects 50 or 90% of the infected mice, respectively) were determined for cefepime-**2** and meropenem-**3** using a murine peritonitis model. Mice were intraperitoneally infected with one of three different *A.*

baumannii strains (NCTC 13301 carrying bla_{OXA-23} and $bla_{OXA-51-like}$, NCTC 13303 possessing bla_{OXA-26} ($bla_{OXA-24/40-like}$) and $bla_{OXA-51-like}$, and SL46 with bla_{OXA-23} and bla_{OXA-51}); MICs are presented in Table 4. The mice were treated with cefepime, cefepime-**2**, meropenem, meropenem-**3**, tigecycline, or colistin, and survival patterns were monitored for 7 days. The $PD_{50/90}$ for cefepime-**2** ranged between 50 and 100 mg/kg for cefepime and 23.23–52.30 mg/kg for **2** (Table 4). Remarkably, the cefepime-**2** $PD_{50/90}$ provides just 25% exposure compared to the exposures at the selected clinical dose.[29,30] For meropenem-**3**, the $PD_{50/90}$'s were 25–50 mg/kg for meropenem and 16.30–66.17 mg/kg for **3** (Table 4). Tigecycline, although employed at supra-therapeutic doses (6.25 mg/kg administered as two doses), failed to protect infected mice (Table 4). Considering the colistin MIC values of 0.5—1 μg/mL, colistin appropriately exhibited low $PD_{50/90}$ values (Table 4).[31]

For the in vivo eradication efficacy of cefepime-**2** and meropenem-**3** to be determined, a neutropenic lung infection model was used in which mice were intranasally infected with a clinical isolate of *A. baumannii* SL04 carrying bla_{OXA-23} and bla_{OXA-51}. The MICs for this isolate are as follows: cefepime, 256 μg/mL; **2**, ≥512 μg/mL; cefepime-**2**, 32 μg/mL; imipenem, 64 μg/mL; meropenem, 64 μg/mL; meropenem-**3**, 8 μg/mL; colistin, 2 μg/mL; and tigecycline, 4 μg/mL. Thus, the MIC of cefepime was reduced by 8-fold when in combination with **2**. Two hours post infection, mice were treated by q2h dosing for 24 h by a subcutaneous route. Three hours post last dose (i.e., 27 h postinfection), the murine lungs were removed, and colony forming units (CFUs) were determined. Treatment of infected mice with cefepime (50 mg/kg), meropenem:cilastatin (25–25 mg/kg), and imipenem:cilastatin (25–25 mg/kg) revealed a 0.67–1.31 log increase in bacterial burden as compared to the 2 h count (Figure 7A). Treatment with cefepime-**2** (50–8.33 mg/kg) resulted in a 3 log kill (Figure 7B). Notably, the addition of **2** to cefepime enhanced the bactericidal action of cefepime even at very low dose of 50 mg/kg.[32] Similarly, the addition of **3** at 4.68 mg/kg to meropenem:cilastatin (25–25 mg/kg) resulted in a 2.47 log kill (Figure 7B). Conversely, relebactam at 18.75 mg/kg combined with imipenem:cilastatin at 25 mg/kg resulted in a 0.86 log increase in CFUs (Figure 7B). It is important to note that *A. baumannii* NCTC 13301, SL46 and SL04 produce OXA-23 and OXA-51, which are not inhibited by **2**. Even with higher MICs, the cefepime-**2** combination provided potent in vivo efficacy against these strains based on its BLE mechanism of action.[33] The most significant feature of the BLE mechanism is the augmentation of the pharmacodynamic action of the partner β-lactam antibiotic. In addition, BLEs enhance the arsenal of agents required to overcome β-lactamases. A further challenge in designing novel BLIs also stems from imparting them with structural features, which facilitate their efficient penetration into MDR Gram-negative pathogens. Many contemporary MDR pathogens express effux pumps as well as mutations in the genes encoding various outer membrane proteins. These mechanisms could impact the uptake of some newer BLIs that show potent activity against inhibitor-resistant enzymes. Compound **3**, by virtue of its potent BLI activity for OXA-carbapenemases and ease of penetration, restores the efficacy of meropenem against MDR *A. baumannii*.[31]

CONCLUSIONS

Here, we revealed the biochemical activity of three novel DBOs, compounds **1–3** against some of the most challenging β-lactamases in Gram-negative bacteria (i.e., KPC-2, PDC-3, ADC-7, OXA-23, OXA-24/40, and OXA-48). We also verified in vivo efficacy of cefepime-**2** and meropenem-**3**. Compound **3** was found to extend the kinetic inhibitory profile of DBOs to OXA carbapenemases while maintaining class A and C activity. Compounds **1** and **2** demonstrated increased potency against class C β-lactamases compared to avibactam and relebactam. Compounds **1** and **2** are unique DBOs in that they also target PBPs of many Gram-negative pathogens and have BLE activity. Thus, they work synergistically when paired with an appropriate β-lactam antibiotic and overcome β-lactamase-mediated resistance without the need to inhibit multiple β-lactamases. The addition of compounds **1–3** to our armamentarium would be highly beneficial as the clinically available β-lactams and β-lactam-BLI combinations are not effective against these refractory Gram-negative pathogens. Finally, compounds **1–3** exemplify two divergent strategies in rejuvenating β-lactam antibiotics.

EXPERIMENTAL SECTION

Compound Characterization.

Nuclear magnetic resonance spectra were recorded on a Mercury 400 MHz (Varian Inc.) or 500 MHz (Bruker). The mass spectra were recorded on a TQD mass spectrometer (Waters Corp.) using the electrospray ionization technique. Elemental analysis was conducted on Vario-Micro cube elemental analyzer (Elementar). Water content was determined using Karl-fisher titration method. The purity (>95%) of all of the compounds was established using the high-pressure liquid chromatography method with 5 μm particle size C18 columns (Bonna Agela Technologies for **2** and YMC Technologies for the remaining compounds) maintaining solution at 10 °C.

Synthesis of 1 and 2.

Figure 2A represents construction of BCH backbone intermediate **1b** and **2b** as a result of coupling of corresponding chiral acid hydrazide **1a** or **2a** with sodium salt of DBO nucleus represented by A by using EDC·HCl as a coupling agent in water (~87%, $n = 1$ and 2). Subsequent catalytic hydrogenation (10% Pd/C catalyst) furnished hydroxyl intermediate (**1c**, $n = 1$ or **2c**, $n = 2$) in quantitative yield, which was subjected to sulfonation reaction immediately by using sulfurtrioxide pyridine complex to afford sulfonated intermediate. The sulfonated intermediate was isolated in the form of tetrabutylammonium salt **1d** (60%, $n = 1$) or **2d** (87%, $n = 2$). Finally, removal of the N-Boc group and tetrabutyl ammonium salt was achieved in one step using excess TFA at 0–5 °C. Compounds were purified by crystallizing in aqueous isopropanol to furnish **1** (**1e**, $n = 1$, 60%,), or **2** (**2e**, $n = 2$, 80%).

Synthesis of 3.

Figure 2B represents the synthesis of **3**,[34] where the sodium salt of the DBO core (A) was converted into the mixed anhydride by first treating the sodium salt with triethylamine hydrochloride in dichloromethane and reacting the resulting compound with pivaloyl

chloride in the presence of a base triethylamine at 0–5 °C, to obtain the mixed anhydride, which was as such reacted with a 25% aqueous solution of ammonia in water at –20 °C to obtain the amide (**3a**) as an off-white solid after workup and purification. The amide (**3a**) was dehydrated with trifluoroacetic anhydride in the presence of triethylamine in dichloromethane at –5 °C to RT to obtain the cyano compound (**3b**), which was debenzylated with 10% Pd/C (50% wet) in a 1:1 (v/v) mixture of DMF:DCM (v/v) under a hydrogen atmosphere (50–55 psi) to obtain the hydroxyl compound (**3c**). This compound was then immediately sulfated with the DMF:SO_3 complex to obtain the sulfate, which was isolated as its tetrabutylammonium salt (**3d**) by reacting with tetrabutylammonium acetate. The tetrabutylammonium salt (**3d**) was converted to **3** by passing the salt through a column filled with Indion 225 sodium resin. Compound **3** was obtained as a white solid by lyophylization of the aqueous solution and recrystallization of the dry powder from a mixture of isopropanol and water.

Synthesis of (2S,5R)-6-Sulfooxy-7-oxo-2-[((3R)-pyrrolidine-3-carbonyl)hydrazinocarbonyl]-1,6-diazabicyclo[3.2.1]octane, 1 (1e).—Step 1: (2*S*,5*R*)-6-Benzyloxy-7-oxo-2-[((3*R*)-*N*-Boc-pyrrolidine-3-carbonyl)hydrazinocarbonyl]-1,6-diazabicyclo[3.2.1]octane (**1b**): white solid, 95 g, 88%; ^{1}H NMR ($CDCl_3$) δ 8.61 (br s, 1H), 8.21 (br d, 1H), 7.36–7.43 (m, 5H), 5.04 (d, *J* = 11.2 Hz, 1H), 4.90 (d, *J* =11.6 Hz, 1H), 3.99 (d, *J* = 6.8 Hz, 1H), 3.60–3.70 (m, 1H), 3.48–3.52 (m, 2H), 3.24–3.40 (m, 2H), 3.04–3.18 (m, 2H), 2.98 (t, *J* = 11.6 Hz, 1H), 2.24–2.34 (m, 1H), 2.12 (br s, 2H), 1.91–2.04 (m, 2H), 1.58–1.66 (m, 1H), 1.43 (s, 9H); Mass (M - 1) = 486.3 for $C_{24}H_{33}N_5O_6$; HPLC purity, 98.89%. Step 2: (2*S*,5*R*)-6-Hydroxy-7-oxo-2-[((3*R*)-*N*-Boc-pyrrolidine-3-carbonyl)hydrazinocarbonyl]-1,6-diazabicyclo-[3.2.1]octane (**1c**): white solid, 72 g, quantitative; ^{1}H NMR (400 MHz, DMSO-d_6) δ 9.70–9.90 (m, 3H), 3.76 (d, *J* = 7.6 Hz, 1H), 3.59 (br s, 1H), 3.41–3.46 (m, 1H), 3.18–3.29 (m, 2H), 3.13–3.17 (m, 2H), 2.96–2.99 (m, 2H), 1.82–2.05 (m, 4H), 1.71–1.81 (m, 1H), 1.53–1.71 (m, 1H), 1.37 (s, 9H); Mass (M - 1) = 396.2 for $C_{17}H_{27}N_5O_6$. Step 3: Tetrabutyl ammonium salt of (2*S*,5*R*)-6-sulfooxy-7-oxo-2-[((3*R*)-*N*-Boc-pyrrolidine-3-carbonyl)hydrazinocarbonyl]-1,6-diazabicyclo[3.2.1]octane (**1d**): white foamy solid, 106 g, 87%; ^{1}H NMR (400 MHz, $CDCl_3$) δ 8.76 (br s, 1H), 8.60 (s, 1H), 4.23 (br s, 1H), 3.97 (d, *J* = 8.0 Hz, 1H), 3.58–3.68 (m, 1H), 3.46–3.54 (m, 2H), 3.30–3.34 (m, 1H), 3.22–3.27 (m, 9H), 3.08–3.11 (m, 1H), 12.28–2.33 (m, 1H), 2.10–2.17 (m, 5H), 1.83–1.89 (m, 1H), 1.57–1.71 (m, 9H), 1.36–1.46 (m, 15H), 0.98 (t, 12H); Mass (M - 1) = 476.4 as a free sulfonic acid for $C_{17}H_{26}N_5O_9S{\cdot}N(C_4H_9)_4$. Step 4: Compound **1**: (2*S*,5*R*)-6-Sulfooxy-7-oxo-2-[((3*R*)-pyrrolidine-3-carbonyl)hydrazinocarbonyl]-1,6-diazabicyclo[3.2.1]octane (*1e*): white crystalline solid, 33 g, 60%; ^{1}H NMR (400 MHz, DMSO-d_6, D_2O exchange) δ 4.03 (br s, 1H), 3.85 (d, *J* = 7.2 Hz, 1H), 3.02–3.39 (m, 7H), 2.17–2.22 (m, 1H), 1.99–2.06 (m, 2H), 1.87–1.90 (br s, 1H), 1.70–1.76 (m, 1H), 1.60–1.64 (m, 1H); ^{13}C NMR (100 MHz, DMSO-d_6) δ 171.1, 168.9, 166.1, 58.4, 57.7, 47.0, 46.9, 45.3, 40.1,28.7, 20.6, 18.4; IR (cm^{-1}) 3568, 1746, 1709, 1676, 1279, 1234, 1015; Anal. Calcd for **1** monohydrate $C_{12}H_{19}N_5O_7S.H_2O$ C 36.42, H 5.31, N 17.70; Found C 36.75, H 5.42, N 17.69; Mass (M - 1) = 376.3 for $C_{12}H_{19}N_5O_7S$; HPLC purity, 98.46%; column, 5 μm particle size, 25 cm length YMC ODS AM C18 column (YMC Technologies); mobile phase used was buffer (0.1 M ammonium dihydrogen phosphate in water) and methanol in

gradient mode; detection, 225 nm; column temperature, 25 °C; flow rate, 0.7 mL/min; **1** solution was maintained at 10 °C; specific rotation $[\alpha]^{25}_{D}$ −47.5° (*c* 0.5, water).

Synthesis of (2S,5R)-6-Sulfooxy-7-oxo-2-[((3R)-piperidine-3-carbonyl)hydrazinocarbonyl]-1,6-diazabicyclo[3.2.1]octane 2 (2e).—Step 1: (2*S*,5*R*)-6-Benzyloxy-7-oxo-2-[((3*R*)-*N*-Boc-piperidine-3-carbonyl)hydrazinocarbonyl]-1,6-diazabicyclo[3.2.1]octane (**2b**): To a clear solution of sodium (2*S*,5*R*)-7-oxo-6-benzyloxy-1,6-diazabicyclo-[3.2.1]octane-2-carboxylate (A, 200 g, 0.67 mol) in water (3.2 L) was added (*R*)-*N*-Boc-piperidine-3-carboxylic acid hydrazide [**2a**, prepared by heating *R*-ethyl-*N*-Boc-nipecotic acid and hydrazine; specific rotation $[\alpha]^{25}_{D}$ −53.5° (*c* 0.5, methanol); HPLC purity, 99%, 171 g, 0.70 mol]. The resulting suspension was treated with EDC·HCl (193 g, 1.01 mol) and HOBt (90.6 g, 0.67 mol) with vigorous stirring at ambient temperature. The resultant precipitation was filtered after 16 h, and the wet cake was suspended in warm water. The suspension was filtered and dried under a vacuum at 45 °C to furnish coupled intermediate **2b** as a white powder in 270 g quantity in 87% yield. NMR analyses are shown below, and based on the mass, the product was identified as $C_{25}H_{35}N_5O_6$: ^{1}H NMR (400 MHz, $CDCl_3$) δ 8.42 (br s, 2H), 7.37–7.43 (m, 5H), 5.06 (d, *J* = 12.2 Hz, 1H), 4.91 (d, *J* = 12.2 Hz, 1H), 4.00 (d, *J* = 7.6 Hz, 1H), 3.84 (br s, 1H), 3.52–3.76 (m, 1H), 3.40–3.51 (m, 1H), 3.30 (br s, 1H), 3.18 (br d, *J* = 12.0 Hz, 1H), 3.06 (br d, *J* = 12.0 Hz, 1H), 2.43 (m, 1H), 2.29–2.34 (m, 1H), 1.88–2.00 (m, 4H), 1.60–1.77 (m, 4H), 1.44 (s, 9H); ^{13}C NMR (100 MHz, DMSO-d_6) δ 172.3, 168.6, 167.3, 154.9, 135.4, 129.2, 128.7, 128.5, 80.1, 78.2, 59.1, 57.7, 47.7, 45.5, 44.5, 40.8, 28.3, 27.5, 24.0, 20.6, 17.4; IR (cm^{-1}) 2974, 1751, 1670, 1244, 1153, 1024; Anal. Calcd for $C_{25}H_{35}N_5O_6$ C 59.86, H 13.96, N 7.03; Found C 60.26, H 14.20, N 7.20. Mass (M + 1) = 502.3 for $C_{25}H_{35}N_5O_6$; HPLC purity, 98.4%. Step 2: (2*S*,5*R*)-6-Hydroxy-7-oxo-2-[((3*R*)-N-Boc-piperidine-3-carbonyl)hydrazinocarbonyl]-1,6-diazabicyclo[3. 2.1]octane (**2c**): Coupled intermediate **2b** from step 1 (153 g, 0.305 mol) was dissolved in methanol (1.53 L). To this clear solution was added 10% Pd/C (15.3 g, 50% wet) catalyst. The suspension was purged with hydrogen gas for 3 h at 35 °C under stirring. The catalyst was filtered, and the filtrate was evaporated under vacuum below 40 °C to provide a crude residue. The residue was triturated with hexanes. The solid was filtered to furnish hydroxyl intermediate **2c** in 125 g quantity as a white solid in quantitative yield. The intermediate was used immediately for the next reaction: ^{1}H NMR (500 MHz, DMSO-d_6) δ 9.75 (br s, 3H), 3.90 (br d, 2H), 3.77 (d, *J* = 10 Hz, 1H), 3.60 (br s, 1H), 3.20 (d, *J* = 10 Hz, 1H), 2.96–3.01 (m, 1H), 2.60–2.73 (m, 1H), 2.28–2.30 (m, 1H), 2.01–2.04 (m, 1H), 1.88–1.94 (m, 1H), 1.72–1.82 (m, 3H),1.51–1.68 (m, 4H), 1.40 (s, 9H); ^{13}C NMR (125 MHz, DMSO-d_6) δ 171.87, 168.97, 166.83, 153.79, 78.78, 58.57. 57.71, 47.09, 40.40, 28.05, 27.42, 20.33, 18.29; Mass (M – 1) = 410.3 for $C_{18}H_{29}N_5O_6$; HPLC purity, 96.34%. Step 3: Tetrabutyl ammonium salt of (2*S*,5*R*)-6-sulfooxy-7-oxo-2-[((3*R*)-*N*-Boc-piperidine-3-carbonyl)hydrazinocarbonyl]-1,6-diazabicyclo[3.2.1]octane (**2d**): To the clear mixture of hydroxyl intermediate **2c** (113 g, 0.274 mol) in dichloromethane (1.13 L) was added triethylamine (77 mL, 0.548 mol) followed by sulfurtrioxide pyridine complex (57 g, 0.356 mol) at 35 °C. The reaction mixture was stirred for 3 h, and 0.5 M aqueous potassium dihydrogen phosphate (1.13 L) was added followed by ethyl acetate (2.26 L). The aqueous layer was washed with a dichloromethane:ethyl acetate mixture (1:2 v/v, 2.26 L twice). The aqueous layer was stirred

with solid tetrabutyl ammonium hydrogen sulfate (84 g, 0.247 mol) for 3 h. The mixture was extracted with dichloromethane (1.13 L). The organic layer was evaporated under a vacuum to provide crude TBA salt. It was purified on a short silica gel column to provide pure intermediate **2d** as a foamy white solid in 122 g (60%) quantity: ^{1}H NMR (400 MHz, $CDCl_3$) δ 8.54 (br s, 2H), 4.31 (br s, 1H), 3.98 (d, J = 8 Hz, 2H), 3.18–3.37 (m, 12H), 2.45 (br s, 1H), 2.32–2.37 (m, 1H), 2.10–2.20 (br m, 1H), 1.83–1.96 (m, 5H), 1.62–1.73 (m, 10H), 1.26–1.49 (m, 18H), 1.00 (t, 12H); ^{13}C NMR (100 MHz, $CDCl_3$) δ 172.32, 168.50, 165.82, 154.78, 60.22, 59.30, 58.40, 57.79, 47.86, 40.68, 28.22, 23.96, 23.70, 20.49, 19.49, 17.28, 13.49; Mass (M – 1) = 490.4 as a free sulfonic acid for $C_{18}H_{28}N_5O_9S{\cdot}N(C_4H_9)_4$; HPLC purity, 96.3%. Step 4: Compound **2**: (2*S*,5*R*)-6-sulfooxy-7-oxo-2-[((3*R*)-piperidine-3-carbonyl)hydrazinocarbonyl]-1,6-diazabicyclo[3.2.1]octane (**2e**): To the clear solution of TBA salt intermediate **2d** (113 g, 0.154 mol) in dichloromethane (280 mL) was added trifluoroacetic acid (280 mL) between 0 and 5 °C via addition funnel. The excess trifluoroacetic acid and solvent were evaporated under a vacuum below 40 °C to provide a pale yellow oily residue, which was triturated with methyl *tert*-butyl ether (2.25 L × 2). The precipitate was filtered and suspended in acetone (1.130 L), and the pH of suspension was adjusted to 5.5–6.5 (an aliquot of the slurry was taken out and made a clear solution by adding water prior to measuring the pH) by adding a 10% solution of sodium-2-ethyl hexanoate in acetone. The suspension was filtered and dried under a vacuum below 40 °C to furnish 65 g of crude **2**. Crude **2** was purified in 15% aqueous isopropanol to provide white crystalline **2** (**2e**) in 48 g quantity in 80% yield: ^{1}H NMR (400 MHz, DMSO-d_6) δ 9.99 (br s, 2H), 8.39 (br s, 2H), 4.03 (br s, 1H), 3.84 (d, J = 6.8 Hz, 1H), 3.12–3.23 (m, 3H), 2.99–3.05 (m, 2H), 2.91 (t, J = 10 Hz, 1H), 2.68 (br m, 1H), 1.99–2.05 (m, 1H), 1.57–1.90 (m, 7H); ^{13}C NMR (100 MHz, DMSO-d_6): δ 171.1, 168.9, 165.9, 58.3, 57.5, 46.9, 44.3, 43.2, 36.9, 25.8, 20.9, 20.5, 18.4; IR (cm^{-1}) 3509, 1749, 1715, 1676, 1279, 1242, 1030; Anal. Calcd for **2** dihydrate $C_{13}H_{21}N_5O_7S{\cdot}2H_2O$ C 36.53, H 5.89, N 16.39; Found C 36.26, H 5.92, N 16.30; Mass (M + 1) = 392.3 for $C_{13}H_{21}N_5O_7S$; HPLC purity, 98.84%; column: 5 μm particle size Unisol C18 column (Bonna Agela Technologies); mobile phase: buffer (0.01 M ammonium dihydrogen phosphate water and pH adjusted to 7.2 ± 0.1 with dilute ammonia solution) and acetonitrile in gradient mode; detection: 225 nm; column temperature, 25 °C; flow rate, 1 mL/min; **2** solution was maintained at 10 °C; specific rotation $[\alpha]^{25}_{D}$ –32.6° (c 0.5, water).

Synthesis of (2S,5R)-1,6-Diazabicyclo[3.2.1]octane-2-carbonitrile-7-oxo-6-(sulfooxy)-monosodium Salt (3).—Step 1: Preparation of (2*S*,5*R*)-6-(benzyloxy)-7-oxo-1,6-diazabicyclo[3.2.1]octane-2-carboxamide (**3a**): Triethylamine hydrochloride (104 g, 0.755 mol) was added to a suspension of sodium (2*S*,5*R*)-6-(benzyloxy)-7-oxo-1,6-diazabicyclo[3.2.1]octane-2-carboxylate A (150 g, 0.503 mol) in DCM (1.5 L) under stirring at 30 °C, and after 1 h, triethylamine (70 mL,0.503 mol) was added followed by dropwise addition of pivaloyl chloride (74 mL, 0.603 mol) at 0–5 °C and stirring continued further for 1 h. The reaction mixture was cooled to –20 °C, and aqueous ammonia (103 mL, 1.51 mol) was slowly added. After 30 min of stirring at –20 °C, water (1.5 L) was added, and the two layers separated. The aqueous layer was extracted with fresh DCM (750 mL). The combined organic layer was dried over anhydrous Na_2SO_4 and evaporated under reduced pressure (200 mmHg). The concentrate was diluted with *n*-butyl chloride (450 mL), and the mixture was

stirred for 2 h. The separated solid was filtered, and the solid residue was washed with fresh *n*-butyl chloride (100 mL). The solid was dried under reduced pressure (4 mmHg) to obtain the product (**3a**) as a white solid: 55 g; yield, 40%; mp 170–172 °C; ^{1}H NMR (500 MHz, $CDCl_3$) δ 7.42–7.27 (m, 5H), 6.60 (1H, s), 5.71 (s, 1H), 5.06 (d, 1H, J = 10 Hz), 4.91 (d, 1H, J = 10 Hz), 4.95 (d, 1H, J = 10 Hz), 3.32 (s, 1H), 3.04 (d, 1H, J = 10 Hz), 2.77 (d, 1H, J = 10 Hz), 2.37–2.33 (1H, m), 2.02–1.92 (m, 2H), 1.62 (1H, m); Mass (M + 1) = 276 for $C_{14}H_{17}N_3O_3$; HPLC purity, 99.11%. Step 2: Synthesis of (2*S*,5*R*)-6-(benzyloxy)-7-oxo-1,6-diazabicyclo[3.2.1]octane-2-carbonitrile (**3b**): Trifluoroacetic anhydride (48 mL, 0.340 mol) was slowly added to a solution of (2*S*,5*R*)-6-(benzyloxy)-7-oxo-1,6-diazabicyclo[3.2.1]-octane-2-carboxamide, **3a** (47.0 g, 0.170 mol), in DCM (1430 mL) containing triethylamine (107 mL, 0.765 mol) at –5 °C under stirring. After 2 h of stirring at –5 °C, water (1450 mL) was added to the reaction mixture and stirring continued for 15 min. The organic layer was separated and washed with saturated sodium bicarbonate solution (470 mL) and brine (470 mL), dried over anhydrous Na_2SO_4, and evaporated under reduced pressure (200 mmHg). The crude thus obtained was purified by column chromatography over silica gel (60–120 mesh) using 10–20% v/v mixtures of acetone:hexane as an eluent. Evaporation of the solvent from the combined fractions gave the product (**3b**, 32 g) as a buff-colored solid: yield, 74%; mp 80–82 °C; ^{1}H NMR (500 MHz, DMSO-d_6) δ 7.41–7.38 (m, 5H), 5.06–5.04 (d, 1H, J = 8 Hz), 4.91–4.89 (d, 1H, J = 8 Hz), 4.38–4.37 (d, 1H, J = 4 Hz), 3.37–3.36 (t, 1H, J = 4 Hz), 3.30–3.27 (d,1H, J = 12 Hz), 3.16–3.16 (m, 1H), 2.31–2.27 (m, 1H), 2.13–2.12 (m, 1H), 1.89–1.81 (m, 2H); Mass (M + 1) = 258 for $C_{14}H_{15}N_3O_2$; HPLC purity, 100%. Step 3: Synthesis of (2*S*,5*R*)-6-hydroxy-7-oxo-1,6-diazabicyclo-[3.2.1]octane-2-carbonitrile (**3c**): A solution of (2*S*,5*R*)-6-(benzyloxy)-7-oxo-1,6-diazabicyclo[3.2.1]octane-2-carbonitrile **3b** (32 g, 0.124 mol) in a mixture of DMF:DCM (1:1, 160 mL:160 mL) containing 10% Pd/C (4.6 g, 50% wet) was hydrogenated at 50–55 psi for 2 h at 25 °C. The resulting mixture was filtered through a Celite pad, and the residue was washed with DMF:DCM (1:1, 25 mL:25 mL). The solvent from the combined filtrate was evaporated under reduced pressure to obtain the product as an oil, which was used as such for the next reaction without further purification (20.66 g; ~100% yield). A small quantity was purified by column chromatography over silica gel (60–120 mesh) and using 30–35% v/v mixture of acetone:hexane as the eluent. Evaporation of the solvent from the combined fractions gave the product (**3c**) as a pale yellow solid: mp 135–140 °C (dec); ^{1}H NMR (500 MHz, DMSO-d_6) δ 9.97 (s, 1H), 4.52–4.50 (d, 1H, J = 8 Hz), 3.69 (s, 1H), 3.19 (s, 2H), 2.01–2.00 (m, 2H), 1.86–1.83 (m, 2H); Mass (M – 1) = 166.1 for $C_7H_9N_3O_2$; HPLC purity, 99.7%. Step 4: Synthesis of (2*S*,5*R*)-6-(sulfooxy)-7-oxo-1,6-diazabicyclo-[3.2.1]octane-2-carbonitrile tetrabutylammonium salt (**3d**): To a stirred and cooled (5–10 °C) solution of (2*S*,5*R*)-6-hydroxy-7-oxo-1,6-diazabicyclo[3.2.1]octane-2-carbonitrile **3c** (20.66 g, 0.124 mol) in DMF (160 mL) was added the DMF-SO_3 complex (22.8 g, 0.149 mol) in one portion, and stirring was continued further. After 1 h of stirring, to the resulting reaction mass was slowly added a solution of tetrabutylammonium acetate (48.6 g, 0.161 mol) in water (160 mL). After 1 h of further stirring, the solvent from the reaction mixture was evaporated under reduced pressure to obtain an oily residue. The oily mass was coevaporated with xylene (2 × 200 mL) to obtain a thick mass. This mass was partitioned between dichloromethane (320 mL) and water (320 mL). The organic layer was separated, and the aqueous layer was re-extracted with dichloromethane (160 mL). The combined organic extracts were washed with

water (3 × 160 mL) and dried over anhydrous Na_2SO_4, and the solvent was evaporated under reduced pressure at 35 °C. The residual oily mass was triturated with ether (3 × 160 mL) each time the ether layer was decanted, and finally, the residue was dried under reduced pressure to obtain the product (**3d**) as a pale yellow oil: 52.5 g; yield, 86%; ^{1}H NMR (400 MHz, $CDCl_3$) δ 4.42 (s, 1H), 4.34 (d, 1H, J = 6.8 Hz), 3.45 (d, 1H, J = 12.4 Hz), 3.36 (d, 1H, J = 12.4 Hz), 3.31–3.23 (m, 8H), 2.35–2.20 (2H, m), 1.94–1.81 (2H, m), 1.69–1.56 (8H, m), 1.48–1.39 (8H, m), 1.02–0.98 (12H, m); Mass (M – 1) = 246 as a free sulfonic acid for $C_7H_8N_3O_5S{\cdot}N(C_4H_9)_4$; HPLC purity, 95.24%. Step 5: Synthesis of (2*S*,5*R*)-1,6-diazabicyclo[3.2.1]octane-2-carbonitrile-7-oxo-6-(sulfooxy)-monosodium salt (**3**): A solution of (2*S*,5*R*)-6-(sulfooxy)-7-oxo-1,6-diazabicyclo-[3.2.1]octane-2-carbonitrile tetrabutylammonium salt **3d** (51.5 g, 0.105 mol) in THF (50 mL) was loaded on column packed with Indion 225 Na resin (1200 g) and was eluted using 10% THF in water. The pure fractions were collected, and THF was evaporated under reduced pressure. The aqueous solution was extracted with ethyl acetate (5 × 250 mL), treated with charcoal for decolorization, and filtered. The filtrate was lyophilized, and the powder obtained was recrystallized using isopropanol:water to obtain the product (**3**) as a white solid: 20.5 g; yield, 72%; mp 198–201 °C (dec); ^{1}H NMR (400 MHz, DMSO-d_6) δ 4.56–4.54 (d, 1H, J = 6.8 Hz), 4.09 (s, 1H), 3.31–3.22 (s, 2H), 1.98–1.86 (m, 4H); ^{13}C NMR (400 MHz, DMSO-d_6) δ 163.5 (C = O), 119.1 (CN), 57.3 (CH), 48.6 (CH), 48.0 (CH_2), 22.0 (CH_2), 20.2 (CH_2); IR (cm^{-1}) 3543, 2249, 1751, 1292, 1072, 1020, 1009; Mass (M – 1) = 246 as a free sulfonic acid for $C_7H_8N_3O_5SNa$: HPLC purity, 99.6%; water content, 4.18%; Anal. Calcd for **3**, $C_7H_8N_3O_5SNa$ C 31.23, H 3.0, N 15.61; Found C 30.94, H 3.4, N 15.45; specific rotation $[\alpha]^{25}_D$ –28.7° (*c* 0.5, water).

Plasmids and Strains.

The cloning and/or origins for bla_{KPC-2}, bla_{PDC-3}, and bla_{ADC-7} genes for susceptibility testing and bla_{KPC-2}, bla_{PDC-3}, bla_{ADC-7}, bla_{OXA-23}, and $bla_{OXA-24/40}$ genes (missing the nucleotides encoding their signal peptides) for protein expression were described in the following references.[11,20,35–37] The methods for the generation of the *A. baumannii* ATCC17978 knockout strains have been previously described.[38]

For MIC analysis, the bla_{OXA-48} gene was cloned into the pBC SK (−) vector by amplifying the bla_{OXA-48} coding and upstream promoter regions from *K. pneumoniae* CAV1543 containing bla_{OXA-48}, sequence verified, and transformed into the *E. coli* DH10B.[19] For large-scale protein expression, the bla_{OXA-48} gene without its leader peptide sequence was cloned into the pET24a(+) vector using NdeI and XhoI restriction sites and electroporated into *E. coli* DH10B. The resulting construct was sequence verified and transformed into *E. coli* BL21(DE3) cells for protein expression and purification.

For MIC testing, as OXA-23 and OXA-24/40 do not express well in an *E. coli* background, presumably due to codon usage, another expression strategy was utilized. For bla_{OXA-23}, the *bla* gene and its upstream ISAba1 was amplified from strain AB0057, and for $bla_{OXA-24/40}$, the *bla* gene and its upstream XerC/XerD was amplified from strain *A. baumannii* NM55. The amplified genes were cloned into the Xba1 site of the modified pWH1266 vector (a vector that replicates in *A. baumannii*) in which ampicillin resistance was eliminated

(Δbla_{TEM-1}) by inverse PCR, and an Xba1 site was engineered into the vector. Once the proper sequence was confirmed in the constructs, the clone was transformed into the *A. baumannii* OM2 clinical isolate. To reduce the ampicillin MIC of the OM2 strain, the native bla_{ADC} gene was knocked out. A 3 kb fragment including the bla_{ADC} gene and ~1 kb flanking sequence upstream and downstream of bla_{ADC} was amplified out of OM2 and cloned into pCR-XL-TOPO. The bla_{ADC} gene in the pCR-XL-TOPO clone was removed by inverse PCR, and a tobramycin resistance gene was put in its place. This plasmid was used to generate the bla_{ADC} knockout. Linearized bla_{ADC} knockout plasmid was electroporated into OM2 cells with selection on tobramycin. Colonies that grew on tobramycin were PCR screened for the tobramycin resistance gene to ensure that they were not breakthrough colonies. PCR using a primer upstream of the area used to make the bla_{ADC} construct and a second primer residing in the tobramycin resistance gene was performed to show integration into the desired location. Finally, PCR to amplify the bla_{ADC} gene was negative, demonstrating that the bla_{ADC} gene was successfully knocked out. Note: The bla_{ADC} knockout of OM2 still contains bla_{OXA-51}. Numerous attempts to knock out the bla_{OXA-51} gene were unsuccessful. It is unknown if other β-lactamases are present in OM2.

Protein Purification for Kinetic Assays and Mass Spectrometry.

The purification of KPC-2, ADC-7, PDC-3, and OXA-23 was previously described.[11,20,36,37] OXA-24/40 and OXA-48 were purified according to the following protocols.

The OXA-24/40 β-lactamase was purified as follows. *E. coli* BL21(DE3) containing the $bla_{OXA-24/40}$ pET24 (+) construct was grown in SOB containing 50 μg/mL of kanamycin at 37 °C with shaking to achieve an OD_{600} of 0.8. IPTG was added to the culture to a final concentration of 0.2 mM, and the culture was grown for three more hours. The cells were centrifuged and frozen at −20 °C. Pellets were thawed and suspended in 50 mM Tris-HCl, pH 7.4 with lysozyme (40 μg/mL), benzonuclease, and 1 mM $MgSO_4$. Cellular debris was removed by centrifugation, and the lysate was subjected to preparative isoelectric focusing (pIEF) overnight. The location of OXA-24/40 on the pIEF gel was determined using a nitrocefin (NCF; Becton, Dickinson and Company) overlay. OXA-24/40 was further purified by SEC using a HiLoad 16/60 Superdex 75 column (GE Healthcare Life Science). The OXA-48 β-lactamase was purified from *E. coli* BL21(DE3) containing the bla_{OXA-48}/pET24 (+) construct as described above for OXA-24/40.

Steady-State Inhibitor Kinetics.

For determining the inhibitory potential of compounds **1–3** against select class A, C, and D β-lactamases, steady-state inhibition kinetics were conducted using an Agilent 8453 Diode Array spectrophotometer. Class A and C β-lactamases were tested in 10 mM phosphate-buffered saline, pH 7.4, and 50 mM sodium phosphate buffer, pH 7.2 (supplemented with 20 mM sodium bicarbonate) was used for class D β-lactamases.[39] The proposed interactions between β-lactamases and DBOs is depicted in Figure 3A.

As an initial screen for inhibiton, a direct competition assay was performed to estimate the Michaelis constant, $K_{i\ app}$, of the inhibitor. If the $K_{i\ app}$ value was >100 μM, further biochemical analyses were not pursued. We used a final concentration of 50–100 μM (or 3–5

× K_m) of nitrocefin (ncf) as the indicator substrate and nM concentrations of β-lactamase in these determinations. The data were analyzed according to eq 1 to account for the affinity of nitrocefin for the β-lactamase

$$K_{i\,app}(\text{corrected}) = K_{i\,app}(\text{observed})/(1 + [S]/K_m\,\text{nitrocefin}) \quad (1)$$

where [*S*] is the concentration of nitrocefin.

The second-order rate constant for enzyme and inhibitor complex inactivation, k_2/K, was measured directly by monitoring the reaction time courses in the presence of inhibitor. A fixed concentration of enzyme, nitrocefin, and increasing nM concentrations of BLI or BLE were used in each assay. Progress curves were fit to eq 2 to obtain the observed rate constant for inactivation (k_{obs})

$$y = V_f \cdot x + (V_0 - V_f) \cdot [1 - \exp(-k_{obs} \cdot X)]/k_{obs} + A_0 \quad (2)$$

where V_f is the final velocity, V_0 is the initial velocity, and A_0 is the initial absorbance at wavelength 482 nm. Data were plotted as k_{obs} vs [*I*]. The k_2/K values were obtained by correcting the value obtained for the slope of the line (k_2/K observed) for the use of the K_m of ncf for the given enzyme according to eq 3.

$$k_2/K\ (\text{corrected}) = k_2/K\ (\text{observed}) \cdot ([S]/K_m\,\text{ncf}) + 1 \quad (3)$$

The off rate or k_{off} was determined by incubating β-lactamase with DBOs at a concentration of 5× $K_{i\,app}$ for 30 min. Samples were serially diluted, and hydrolysis of 100 μM nitrocefin was measured. The progress curves were fit to a single exponential decay equation.

Partition ratios (k_{cat}/k_{inact} [where k_{inact} is the rate constant of enzyme inactivation]) at 24 h for β-lactamases with inhibitor were obtained by incubating enzyme with increasing concentrations of inhibitor at room temperature. The ratio of inhibitor to enzyme (*I:E*) necessary to inhibit the hydrolysis of NCF by >99% was determined.

Mass Spectrometry.

Electrospray ionization mass spectrometry (ESI-MS) of the intact β-lactamases was performed on a Waters SynaptG2-Si quadrupole-time-of-flight mass spectrometer. The Synapt G2-Si was calibrated with sodium iodide using a 50–2000 *m/z* mass range. This calibration resulted in an error of ±5 amu. After 5 min and 24 h incubation of β-lactamase and inhibitor at a 1:1 ratio, the reactions were terminated by the addition of 0.1% formic acid and 1% acetonitrile. The samples were run using Waters Acquity H class Ultra-Performance Liquid Chromatography (UPLC) on an Acquity UPLC BEH C18 1.7 μm, 2.1 × 100 mm column. The mobile phase consisted of 0.1% formic acid in water. The tune settings for each data run are as follows: capillary voltage, 3.2 kV; sampling cone, 30 V; source

offset, 30; source temperature, 100 °C; desolvation temperature, 450 °C; cone gas, 50 L/h; desolvation gas, 600 L/h; and nebulizer bar, 6.0. Spectra will be analyzed using MassLynx v4.1. Data presented are the consensus results from 2–3 experiments.

For determining if any resulting adducts (e.g., −80 amu, see Results and Discussion) were mass spectrometry artifacts, samples were rerun using capillary voltages of 1 or 4.5 kV with the other conditions as described above. In addition, the samples were rerun with the sampling cone at 5, 20, 30, 40, 50, 60, or 70 V with the other conditions as described above.[4]

Acyl Transfer.

To assess if **1–3** recyclize to reform active compound, an acyl-tranfer ESI-MS experiment was conducted using KPC-2 as the donor and TEM-1 as the recipient. Five micromolar KPC-2 was incubated with **1, 2**, or **3** at an equimolar ratio for 1 min. Five micromolar TEM-1 β-lactamase was added to the mixture. At the time points of 15 s and 5 min, reactions were terminated and prepared for ESI-MS as described above.

Protein Purification for Crystallography.

KPC-2 was expressed and purified as described previously.[40,41] The purified KPC-2 protein was concentrated to 10 mg/mL (measured by Bradford assay), aliquoted, and stored at −80 °C until further use for cocrystallization or soaking of the **1, 2,** or **3** inhibitors as described below. OXA-24/40 was expressed and purified as previously described.[23]

Crystallization of Apo KPC-2 and Soaking of 1–3.

KPC-2 crystals were grown in the same crystallization conditions as described previously,[22] which consists of 20% PEG6000, 100 mM citrate pH 4.0, and 100 mM KSCN, yet 10 mM $CdCl_2$ was added as a crystallization additive to improve crystallization. The addition of $CdCl_2$ also favored KPC-2 to crystallize in the *P*1 spacegroup. The protein concentration for crystallization was 10 mg/mL. The soaking solutions were prepared similarly to crystallization conditions at pH 5.0 with the addition of 10 mM inhibitor (**1–3**). The KPC-2 crystals were soaked for 3 h before being cryo-protected with the soaking solution also containing 20% ethylene glycol and subsequently flash frozen in liquid nitrogen prior to data collection.

Cocrystallization of KPC-2 with 1–3.

Prior to cocrystallization, the KPC-2 protein and each inhibitor were incubated for 40 min with a protein to inhibitor molar ratio of 1 to 10 (KPC-2 concentration was 10 mg/mL). The KPC-2:inhibitor cocrystals were crystallized using 200 mM lithium sulfate, 100 mM sodium acetate pH 4.4–4.6, and 28–31% PEG8000. After growing for ~3 days, the cocrystals were mounted and cryo-protected with perfluoropolyether (Hampton Research) prior to flash freezing in liquid nitrogen.

Cocrystallization of OXA-24/40 with 3.

OXA-24/40 was preincubated with **3** overnight with a 1:50 molar ratio of protein to inhibitor. The OXA-24/40:**3** complex was crystallized in 0.2 M calcium acetate, 0.2 M sodium cacodylate pH 6.5, and 18% PEG8000. Crystals were cryo-protected using the mother liquor before freezing in liquid nitrogen prior to data collection.

X-ray Data Collection and Crystallographic Refinement.

Data for the KPC-2:**1, 2**, and **3** complexes were collected at the SSRL beamline. The data for the OXA-24/40:**3** complex were collected at APS. All data sets were processed using AutoXDS scripts,[42,43] and the protein structures were refined using Refmac[44] and Coot programs.[45] The starting protein coordinates for all KPC-2 structures in this study were KPC-2 in complex with 3-NPBA (PDB ID: 3RXX) and for the OXA-24/40 starting structure was 4WM9. The KPC-2 structures have two molecules in the asymmetric structure, whereas there is only 1 molecule in the asymmetric unit in the OXA-24/40 structure. The structures in the two different molecules in each KPC-2 complex structure are very similar so, for the most part, only molecule A will be discussed. The chemical structures of inhibitors and their corresponding parameter and topology files were generated using the PRODRG program.[46] The coordinates were checked using the structure validation program PROCHECK[47] and found to have no outliers in the Ramachandran plot. The coordinates and structure factors of the structures have been deposited with the Protein Data Bank, and the PDB identifiers are listed in Table S1.

Susceptibility Testing.

MICs for various bacterial isolates were determined by broth microdilution method using custom frozen panels (ThermoFisher Scientific, Cleveland, OH) according to the Clinical and Laboratory Standards Institute guidelines.[48,49] Compounds **1–3,** avibactam, relebactam, meropenem, and cefepime were tested alone. Compounds **1–3** were tested at 4 and 8 mg/L, and avibactam and relebactam were tested at 4 mg/L in combination with increasing concentrations of meropenem and cefepime. MICs were performed in triplicate, and modal values are reported.

Murine Peritonitis Model.

Male and female Swiss albino mice were intraperitoneally infected with a bacterial inoculum (3.5×10^5 to 3×10^6 CFU/mouse) resuspended in 5% hog gastric mucin that resulted in mortality of untreated animals within 24 h. Subcutaneous treatment of drugs was initiated 1 h postinfection for 1 day. Cefepime, cefepime-**2**, meropenem-cilastatin, meropenem-cilastatin-**3**, and tigecycline were given as two doses (3 h apart), and colistin was given three doses (3 h apart). Survival patterns were monitored for 7 days. The $PD_{50/90}$ values were determined by probit analysis. All animal experiments performed in the manuscript were conducted in compliance with Wockhardt Research Centre guidelines.

Neutropenic Murine Lung Infection Model.

Male and female Swiss mice weighing 25–27 g were rendered neutropenic by intraperitoneal administration of cyclophosphamide (150 and 100 mg/kg; 1 and 4 days prior

to infection). Two hours prior to the initiation of antimicrobial therapy, intranasal infection was caused by instilling 80 μL of bacterial suspension (10^5–10^6 $\log_{10}$ CFU/mL) of Indian clinical isolate *A. baumannii* SL04 expressing bla_{OXA-23}. A group of 6 mice were administered humanized doses of cefepime, **2**, and meropenem:cilastatin by subcutaneous route in fractionated regimen. Compound **3** was also administered as fractionated doses in combination with meropenem:cilastatin. Imipenem:cilastatin and relebactam were administered at their simulated clinical doses. Doses were fractionated as q2h regimen. Lungs from all of the animals including untreated animals were harvested 3 h post last dose of q2h regimen and individually homogenized (Homogenizer, IKA Ultra-Turrax T-25) in 3 mL of normal saline. One hundred microliters of this homogenate was diluted serially and plated on trypticase soy agar plates, and the colonies appearing following incubation at 37 °C for 18 h were counted. Bacterial load of untreated animals enumerated at the time of initiation of therapy (2 h post infection) served as a reference count to quantify the magnitude of antibacterial effect realized through various dosing regimens. Bacterial load at initiation of treatment (2 h post infection) was 6.13 ± 0.17 $\log_{10}$ CFU/lung, which increased to 7.62 ± 1.22 $\log_{10}$ CFU/lung at 27 h post infection. All animal experiments performed in the manuscript were conducted in compliance with Wockhardt Research Centre guidelines.

Supplementary Material

Refer to Web version on PubMed Central for supplementary material.

ACKNOWLEDGMENTS

This study was funded by an industry grant from Wockhardt Research Centre (WRC) to K.M.P.W., M.R.J., F.v.d.A., and R.A.B.; WRC also supplied compounds **1–3**, avibactam, and relebactam powders for this work. Research reported in this publication was supported in part by funds and/or facilities provided by the Cleveland Department of Veterans Affairs, the Veterans Affairs Merit Review Program BX002872 (KMP-W), and BX001974 (RAB) from the United States (U.S.) Department of Veterans Affairs Biomedical Laboratory Research and Development Service, and the Geriatric Research Education and Clinical Center VISN 10 to RAB. P.N.R. is also supported by grants from the Merit Review program and a Research Career Scientist Award, both from Department of Veterans Affairs. The contents do not represent the views of the U.S. Department of Veterans Affairs or the United States Government. The National Institute of Allergy and Infectious Diseases (NIAID) of the National Institutes of Health (NIH) under Award Numbers R21AI114508, R01AI100560, R01AI063517, and R01AI072219 to R.A.B. and NIAID of NIH Centers of Excellence for Translational Research (CETR) U19 AI109713 Supplemental Research Project to K.M.P.W are gratefully acknowledged. The content is solely the responsibility of the authors and does not necessarily represent the official views of the National Institutes of Health. We thank the beamline personnel at SSRL for help with data collection. In addition, we thank David Lodowski and APS for help with collecting the OXA-24 data set.

ABBREVIATIONS USED

MDR	multidrug resistant
DBO	diazabicyclooctane
CRE	carbapenem-resistant Enterobacteriaceae
KPC	*Klebsiella pneumoniae* carbapenemase
PDC	*Pseudomonas*-derived cephalosporinase
ADC	*Acinetobacter*-derived cephalosporinase

BLI	β-lactamase inhibitors
BLE	β-lactam enhancer
PBP	pencillin binding protein
IRT	inhibitor-resistant TEM
IRS	inhibitor-resistant SHV
SAR	structure–activity relationships
BCH	bicyclohydrazide
MIC	minimum inhibitory concentration
ColS	colisitin susceptible
ColR	colistin resistant
RND	resistance-nodulation-division
MFP	membrane fusion protein
OMP	outer membrane protein
CFU	colony forming units
pIEF	preparative isoelectric focusing
NCF	nitrocefin

REFERENCES

(1).) Tacconelli E; Carrara E; Savoldi A; Harbarth S; Mendelson M; Monnet DL; Pulcini C; Kahlmeter G; Kluytmans J; Carmeli Y; Ouellette M; Outterson K; Patel J; Cavaleri M; Cox EM; Houchens CR; Grayson ML; Hansen P; Singh N; Theuretzbacher U; Magrini N; Group, W. H. O. P. P. L. W.. Discovery, research, and development of new antibiotics: the WHO priority list of antibiotic-resistant bacteria and tuberculosis. Lancet Infect Dis 2018, 18, 318–327. [PubMed: 29276051]

(2).) Papp-Wallace KM; Bonomo RA New β-lactamase inhibitors in the clinic. Infectious disease clinics of North America 2016, 30, 441–464. [PubMed: 27208767]

(3).) Bonomo RA; Liu J; Chen Y; Ng L; Hujer AM; Anderson VE Inactivation of CMY-2 β-lactamase by tazobactam: initial mass spectroscopic characterization. Biochim. Biophys. Acta, Protein Struct. Mol. Enzymol 2001, 1547, 196–205.

(4).) Ehmann DE; Jahic H; Ross PL; Gu RF; Hu J; Durand-Réville TF; Lahiri S; Thresher J; Livchak S; Gao N; Palmer T; Walkup GK; Fisher SL Kinetics of avibactam inhibition against class A, C, and D β-lactamases. J. Biol. Chem 2013, 288, 27960–27971. [PubMed: 23913691]

(5).) Ehmann DE; Jahic H; Ross PL; Gu RF; Hu J; Kern G; Walkup GK; Fisher SL Avibactam is a covalent, reversible, non-β-lactam β-lactamase inhibitor. Proc. Natl. Acad. Sci. U. S. A 2012, 109, 11663–11668. [PubMed: 22753474]

(6).) King DT; King AM; Lal SM; Wright GD; Strynadka NMolecular C mechanism of avibactam-mediated β-lactamase inhibition. ACS Infect. Dis 2015, 1, 175–184. [PubMed: 27622530]

(7).) Lahiri SD; Walkup GK; Whiteaker JD; Palmer T; McCormack K; Tanudra MA; Nash TJ; Thresher J; Johnstone MR; Hajec L; Livchak S; McLaughlin RE; Alm RA Selection and molecular characterization of ceftazidime/avibactam-resistant mutants in *Pseudomonas*

aeruginosa strains containing derepressed AmpC. J. Antimicrob. Chemother 2015, 70, 1650–1658. [PubMed: 25645206]

(8).) King AM; King DT; French S; Brouillette E; Asli A; Alexander JA; Vuckovic M; Maiti SN; Parr TR, Jr.; Brown ED; Malouin F; Strynadka NC; Wright GD Structural and kinetic characterization of diazabicyclooctanes as dual inhibitors of both serine-β-lactamases and penicillin-binding proteins. ACS Chem. Biol 2016, 11, 864–868. [PubMed: 26731698]

(9).) Mushtaq S; Warner M; Livermore DM In vitro activity of ceftazidime+NXL104 against *Pseudomonas aeruginosa* and other nonfermenters. J. Antimicrob. Chemother 2010, 65, 2376–2381. [PubMed: 20801783]

(10).) Blizzard TA; Chen H; Kim S; Wu J; Bodner R; Gude C; Imbriglio J; Young K; Park YW; Ogawa A; Raghoobar S; Hairston N; Painter RE; Wisniewski D; Scapin G; Fitzgerald P; Sharma N; Lu J; Ha S; Hermes J; Hammond ML Discovery of MK-7655, a β-lactamase inhibitor for combination with Primaxin(R). Bioorg. Med. Chem. Lett 2014, 24, 780–785. [PubMed: 24433862]

(11).) Moya B; Barcelo IM; Bhagwat S; Patel M; Bou G; Papp-Wallace KM; Bonomo RA; Oliver A WCK 5107 (Zidebactam) and WCK 5153 are novel inhibitors of PBP2 showing potent ″β-lactam enhancer″ activity against *Pseudomonas aeruginosa*, including multidrug-resistant metallo-β-lactamase-producing high-risk clones. Antimicrob. Agents Chemother 2017, 61 (e02529–16), 1–12.

(12).) Morinaka A; Tsutsumi Y; Yamada M; Suzuki K; Watanabe T; Abe T; Furuuchi T; Inamura S; Sakamaki Y; Mitsuhashi N; Ida T; Livermore DM OP0595, a new diazabicyclooctane: mode of action as a serine β-lactamase inhibitor, antibiotic and β-lactam 'enhancer'. J. Antimicrob. Chemother 2015, 70, 2779–2786. [PubMed: 26089439]

(13).) Durand-Reville TF; Guler S; Comita-Prevoir J; Chen B; Bifulco N; Huynh H; Lahiri S; Shapiro AB; McLeod SM; Carter NM; Moussa SH; Velez-Vega C; Olivier NB; McLaughlin R; Gao N; Thresher J; Palmer T; Andrews B; Giacobbe RA; Newman JV; Ehmann DE; de Jonge B; O'Donnell J; Mueller JP; Tommasi RA; Miller AA ETX2514 is a broad-spectrum β-lactamase inhibitor for the treatment of drug-resistant Gram-negative bacteria including Acinetobacter baumannii. Nat. Microbiol 2017, 2 (17104), 1–10.

(14).) Mushtaq S; Vickers A; Woodford N; Livermore DM WCK 4234, a novel diazabicyclooctane potentiating carbapenems against Enterobacteriaceae, *Pseudomonas and Acinetobacter* with class A, C and D β-lactamases. J. Antimicrob. Chemother 2017, 72, 1688–1695. [PubMed: 28333319]

(15).) Deshpande PK; Bhavsar SB; Joshi SN; Pawar SS; Kale RP; Mishra AM; Jadhav SB; Pavase LP; Gupta SV; Yeole RD; Rane VP; Ahirrao VK; Bhagwat SS; Patel MV F-479: WCK 5107 (Zidebactam, ZID): Structure activity relationship (SAR) of novel bicyclo acyl hydrazide (BCH) pharmacophore active against Gram negative including Pseudomonas aeruginosa. In ASM Microbe; Boston, MA, 2016.

(16).) Pawar SS; Jadhav SB; Mishra AM; Rane VP; Bhawsar S; Deshpande PK; Yeole RD; Patel MV A Process for Preparation of (2S, 5R)-7-Oxo-6-Sulphooxy-2-[((3R)-pPyrrolidine-3-Carbonyl)-Hydrazino Carbonyl]-1,6-Diaza-Bicyclo[3.2.1]octane. US 20160002234A1, 2014.

(17).) Joshi S; Jadhav SB; Rane VP; Bhawsar S; Deshpande PK; Yeole RD; Patel MV A Process for Preparation of (2S, 5R)-6-Sulphooxy-7-Oxo-2-[((3R)-Piperidine-3-Carbonyl)-Hydrazino Carbonyl]-1,6-Diaza-Bicyclo[3.2.1] octane. WO 2015110885A1, 2014.

(18).) Fleming FF; Yao L; Ravikumar PC; Funk L; Shook BC Nitrile-containing pharmaceuticals: efficacious roles of the nitrile pharmacophore. J. Med. Chem 2010, 53, 7902–7917. [PubMed: 20804202]

(19).) Mathers AJ; Hazen KC; Carroll J; Yeh AJ; Cox HL; Bonomo RA; Sifri CD First clinical cases of OXA-48-producing carbapenem-resistant *Klebsiella pneumoniae* in the United States: the ″menace″ arrives in the new world. J. Clin Microbiol 2013, 51, 680–683. [PubMed: 23175248]

(20).) Papp-Wallace KM; Bethel CR; Distler AM; Kasuboski C; Taracila M; Bonomo RA Inhibitor resistance in the KPC-2 β-lactamase, a preeminent property of this class A β-lactamase. Antimicrob. Agents Chemother. 2010, 54, 890–897. [PubMed: 20008772]

(21).) Ehmann DE; Jahic H; Ross PL; Gu RF; Hu J; Durand-Reville TF; Lahiri S; Thresher J; Livchak S; Gao N; Palmer T; Walkup GK; Fisher SL Kinetics of avibactam inhibition against class A, C, and D β-lactamases. J. Biol. Chem 2013, 288, 27960–27971. [PubMed: 23913691]

(22).) Krishnan NP; Nguyen NQ; Papp-Wallace KM; Bonomo RA; van den Akker F Inhibition of Klebsiella β-lactamases (SHV-1 and KPC-2) by avibactam: a structural study. PLoS One 2015, 10, e0136813. [PubMed: 26340563]

(23).) Bou G; Santillana E; Sheri A; Beceiro A; Sampson JM; Kalp M; Bethel CR; Distler AM; Drawz SM; Pagadala SR; van den Akker F; Bonomo RA; Romero A; Buynak JD Design, synthesis, and crystal structures of 6-alkylidene-2′-substituted penicillanic acid sulfones as potent inhibitors of *Acinetobacter baumannii* OXA-24 carbapenemase. J. Am. Chem. Soc 2010, 132, 13320–13331. [PubMed: 20822105]

(24).) Werner JP; Mitchell JM; Taracila MA; Bonomo RA; Powers RA Exploring the potential of boronic acids as inhibitors of OXA-24/40 β-lactamase. Protein Sci 2017, 26, 515–526. [PubMed: 27997706]

(25).) Lahiri SD; Mangani S; Jahic H; Benvenuti M; Durand-Reville TF; De Luca F; Ehmann DE; Rossolini GM; Alm RA; Docquier JD Molecular basis of selective inhibition and slow reversibility of avibactam against class D carbapenemases: a structure-guided study of OXA-24 and OXA-48. ACS Chem. Biol 2015, 10, 591. [PubMed: 25406838]

(26).) Vercheval L; Bauvois C; di Paolo A; Borel F; Ferrer JL; Sauvage E; Matagne A; Frere JM; Charlier P; Galleni M; Kerff F Three factors that modulate the activity of class D β-lactamases and interfere with the post-translational carboxylation of Lys70. Biochem. J 2010, 432, 495–504. [PubMed: 21108605]

(27).) Bou G; Oliver A; Martinez-Beltran J OXA-24, a novel class D β-lactamase with carbapenemase activity in an *Acinetobacter baumannii* clinical strain. Antimicrob. Agents Chemother 2000, 44, 1556–1561. [PubMed: 10817708]

(28).) Winkler ML; Papp-Wallace KM; Hujer AM; Domitrovic TN; Hujer KM; Hurless KN; Tuohy M; Hall G; Bonomo RA Unexpected challenges in treating multidrug-resistant Gram-negative bacteria: resistance to ceftazidime-avibactam in archived isolates of *Pseudomonas aeruginosa*. Antimicrob. Agents Chemother 2015, 59, 1020–1029. [PubMed: 25451057]

(29).) Takalkar SS; Chavan RP; Patel AM; Umarkar KV; Satav JS; Udaykar AP; Kulkarni AM; Zope VS; Bhagwat SS; Patel MV Sunday 441: WCK 5222 [Cefepime (FEP)-WCK 5107 (Zidebactam, ZID)]: Thigh and lung PK/PD studies against higher MIC OXA carbapenamase-expressing *A. baumannii*. In ASM Microbe; Boston, MA, 2016.

(30).) Joshi PR; Khande HN; Takalkar SS; Kulkarni AM; Chavan RP; Zope VS; Palwe SR; Biniwale SS; Bhagwat SS; Patel MV Sunday 440: WCK 5222 [cefepime (FEP)-WCK 5107 (zidebactam, ZID)]: *in vitro* and *in vivo* coverage of OXA-carbapenemases expressing-*Acinetobacter*. In ASM Microbe; Boston, MA, 2016.

(31).) Khande HN; Takalkar SS; Umarkar KV; Kulkarni AM; Joshi PR; Palwe SR; Biniwale SS; Bhagwat SS; Patel MV Monday 424: WCK 5999 (carbapenem-WCK 4234): *in vitro* and *in vivo* activity of novel broader-spectrum β-lactam-β-lactamase inhibitor against Indian OXA carbapenemase expressing *Acinetobacter*. In ASM Microbe; Boston, MA, 2016.

(32).) Bhagwat SS; Takalkar SS; Chavan RP; Friedland HD; Patel MV Saturday 282: WCK 5222 [cefepime (FEP)-WCK 5107 (zidebactam, ZID)]: unravelling sub-MIC PD effects employing *in vivo* dose fractionation studies and translating into MIC based PK/PD target for carbapenem-resistant *A. baumannii*. In ASM Microbe; New Orleans, LA, 2017.

(33).) Bhagwat SS; Takalkar SS; Chavan RP; Friedland HD; Patel MV Saturday 284: WCK 5222 [cefepime (FEP) + WCK 5107 (zidebactam, ZID)]: *in vivo* demonstration of ZID-mediated β-lactam enhancer effect leading to lowering of FEP %f T > MIC against *P. aeruginosa* and *A. baumannii*. In ASM Microbe; New Orleans, LA, 2017.

(34).) Patil VJ; Ravikumar T; Birajdar S; Bhagwat S Nitrogen Containing Compounds and Their Use. WO 2013038330A1, 2013.

(35).) Che T; Bethel CR; Pusztai-Carey M; Bonomo RA; Carey PR The different inhibition mechanisms of OXA-1 and OXA-24 β-lactamases are determined by the stability of active site carboxylated lysine. J. Biol. Chem 2014, 289, 6152–6164. [PubMed: 24443569]

(36).) Drawz SM; Taracila M; Caselli E; Prati F; Bonomo RA Exploring sequence requirements for C(3)/C(4) carboxylate recognition in the *Pseudomonas aeruginosa* cephalosporinase: Insights into plasticity of the AmpC β-lactamase. Protein Sci 2011, 20, 941–958. [PubMed: 21404358]

(37).) Hujer KM; Hamza NS; Hujer AM; Perez F; Helfand MS; Bethel CR; Thomson JM; Anderson VE; Barlow M; Rice LB; Tenover FC; Bonomo RA Identification of a new allelic variant of the *Acinetobacter baumannii* cephalosporinase, ADC-7 β-lactamase: defining a unique family of class C enzymes. Antimicrob. Agents Chemother 2005, 49, 2941–2948. [PubMed: 15980372]

(38).) Knight D; Dimitrova DD; Rudin SD; Bonomo RA; Rather PN Mutations decreasing intrinsic β-lactam resistance are linked to cell division in the nosocomial pathogen *Acinetobacter baumannii*. Antimicrob. Agents Chemother 2016, 60, 3751–3758. [PubMed: 27067318]

(39).) Leonard DA; Hujer AM; Smith BA; Schneider KD; Bethel CR; Hujer KM; Bonomo RA The role of OXA-1 β-lactamase Asp(66) in the stabilization of the active-site carbamate group and in substrate turnover. Biochem. J 2008, 410, 455–462. [PubMed: 18031291]

(40).) Ke W; Bethel CR; Papp-Wallace KM; Pagadala SR; Nottingham M; Fernandez D; Buynak JD; Bonomo RA; van den Akker F Crystal structures of KPC-2 β-lactamase in complex with 3-nitrophenyl boronic acid and the penam sulfone PSR-3—226. Antimicrob. Agents Chemother 2012, 56, 2713–2718. [PubMed: 22330909]

(41).) Ke W; Bethel CR; Thomson JM; Bonomo RA; van den Akker F Crystal structure of KPC-2: insights into carbapenemase activity in class A β-lactamases. Biochemistry 2007, 46, 5732–5740. [PubMed: 17441734]

(42).) Gonzalez A, Tsay Y A Quick XDS Tutorial for SSRL. http://smb.slac.stanford.edu/facilities/software/xds/#autoxds_script (accessed January 1, 2016).

(43).) Kabsch W Xds. Acta Crystallogr., Sect. D: Biol. Crystallogr 2010, 66, 125–132. [PubMed: 20124692]

(44).) Murshudov GN; Vagin AA; Dodson EJ Refinement of macromolecular structures by the maximum-likelihood method. Acta Crystallogr., Sect. D: Biol. Crystallogr 1997, 53, 240–255. [PubMed: 15299926]

(45).) Emsley P; Cowtan K Coot: model-building tools for molecular graphics. Acta Crystallogr., Sect. D: Biol. Crystallogr 2004, 60, 2126–2132. [PubMed: 15572765]

(46).) Schuttelkopf AW; van Aalten DM PRODRG: a tool for high-throughput crystallography of protein-ligand complexes. Acta Crystallogr., Sect. D: Biol. Crystallogr 2004, 60, 1355–1363. [PubMed: 15272157]

(47).) Laskowski RA; MacArthur MW; Moss DS; Thornton JM PROCHECK - a program to check the stereochemical quality of protein structures. J. Appl. Crystallogr 1993, 26, 283–291.

(48).) Wu G; Robertson DH; Brooks CL r.; Vieth, M. Detailed analysis of grid-based molecular docking: A case study of CDOCKER-A CHARMm-based MD docking algorithm. J. Comput. Chem 2003, 24, 1549–1562. [PubMed: 12925999]

(49).) Drawz SM; Taracila M; Caselli E; Prati F; Bonomo RA Exploring sequence requirements for C3/C4 carboxylate recognition in the *Pseudomonas aeruginosa* cephalosporinase: Insights into plasticity of the AmpC β-Lactamase. Protein Sci 2011, 20, 941–958. [PubMed: 21404358]

(50).) Hori T; Nakano M; Kimura Y; Murakami K Pharmacokinetics and tissue penetration of a new carbapenem, doripenem, intravenously administered to laboratory animals. In Vivo 2006, 20, 91–96. [PubMed: 16433034]

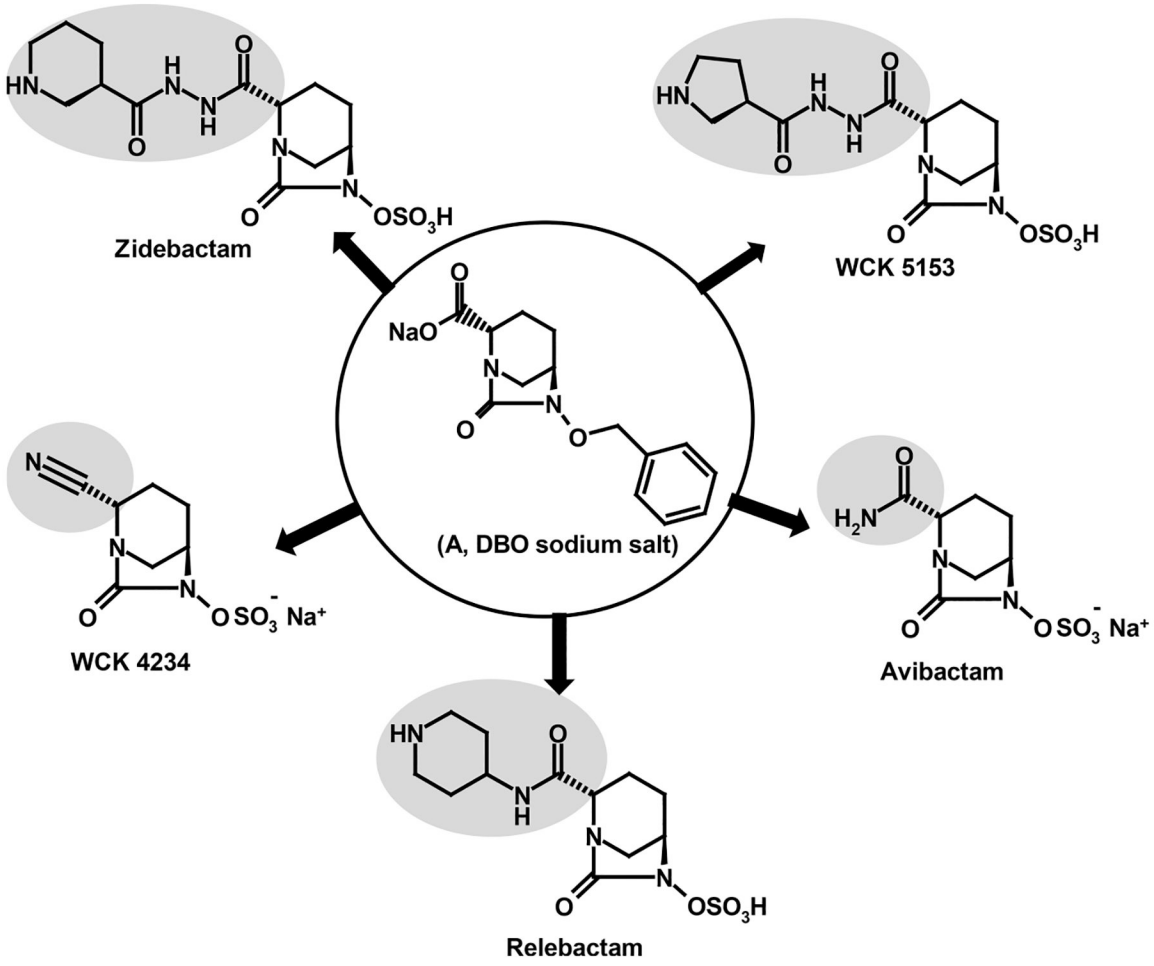

Figure 1.
Structures of DBOs used in this study. R^1 side chain is highlighted by a gray circle.

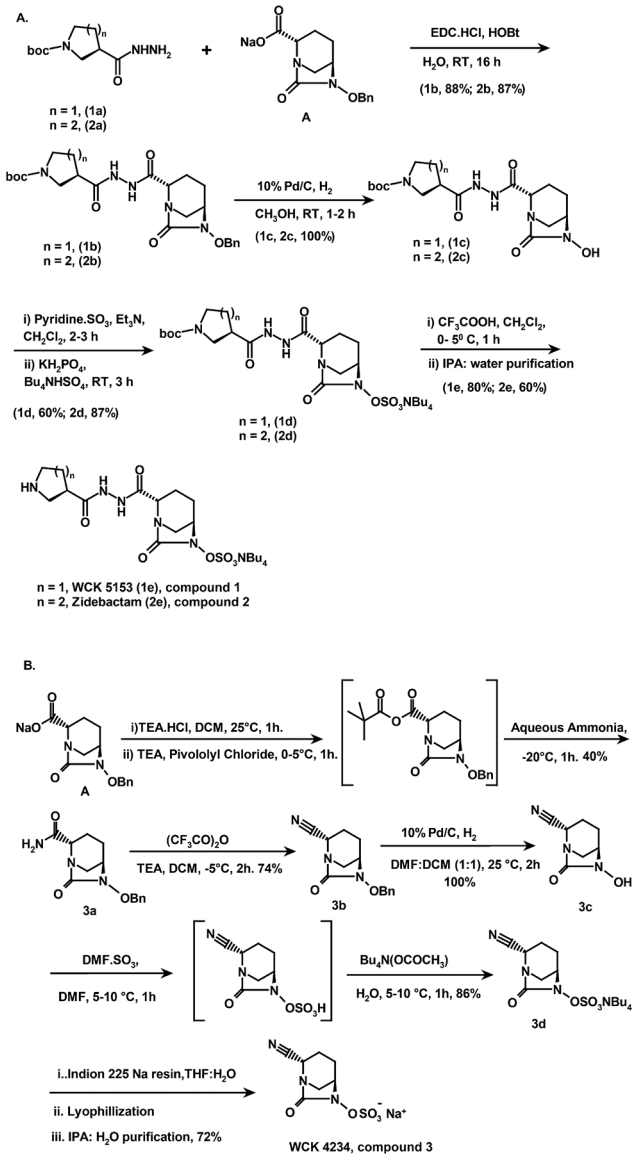

Figure 2.
Syntheses of (A) **1** and **2** and (B) **3**.

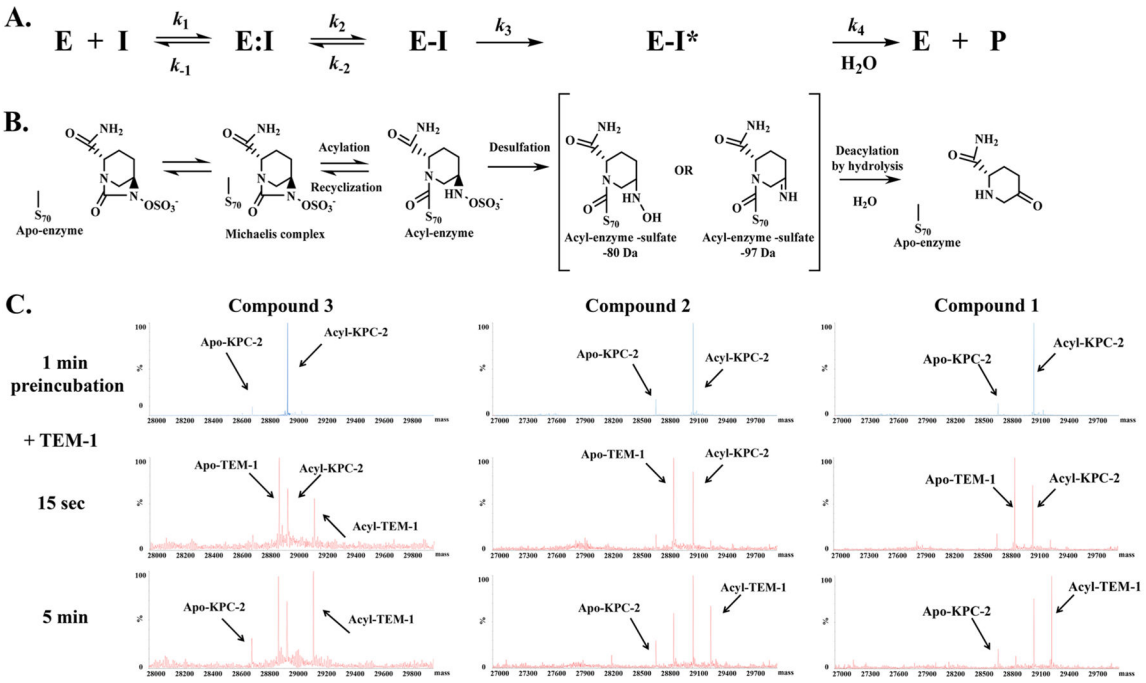

Figure 3.

(A) Scheme representing the interactions of β-lactamases with DBOs. In this model, formation of the noncovalent complex, enzyme:inhibitor (E:I) is represented by the dissociation constant, K_d, which is equivalent to k_{-1}/k_1. k_2 is the first order rate constant for the acylation step or formation of E-I. k_{-2} is the first order rate constant for the recyclization step or reformation of E:I. Reported rarely to date, some DBOs undergo a desulfation reaction; k_3 is the first order rate constant for desulfation to form E:I*, where I* is the desulfated DBO. The desulfated DBO may undergo complete hydrolysis; the hydrolysis, which forms free E and product (P) is represented by the first order rate constant k_4. (B) Chemical representation of (A) using avibactam. (C) Acyl-transfer mass spectrometry with **3** (left), **2** (center), and **1** (right). Each DBO was preincubated with KPC-2 at a 1:1 E:I ratio for 1 min (data in top panels in blue) and used for mass spectrometry; then, TEM-1 was added, incubated for 15 s or 5 min (data in center and bottom panels in red), and used for mass spectrometry.

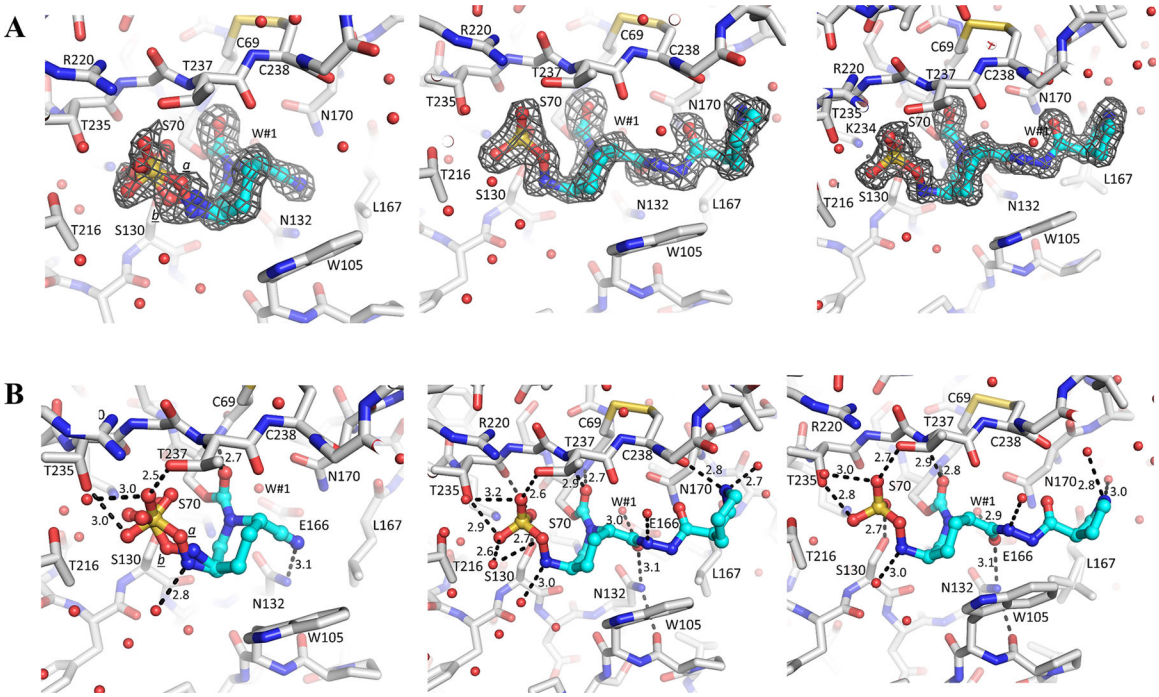

Figure 4.

(A) Electron density of compounds **1–3** bound in the active site of KPC-2. Shown are unbiased omit $|F_o|$-$|F_c|$ electron density with the ligand removed from refinement and map calculations. Left, **3** bound to KPC-2; center, **2** bound to KPC-2; right, **1** bound to KPC-2. Compounds **1–3** are shown in blue carbon atom ball-and-stick representation, and the protein is depicted in gray carbon atom stick representation. Electron density is contoured at the 3σ level, and data sets are from inhibitor-soaked KPC-2 crystals. The sulfate moiety of **3** was observed to be in two conformations (0.6 and 0.4 occupancy conformations labeled *a* and *b*, respectively). (B) Compounds **1–3** bound to the active site of KPC-2. Left, **3** bound to KPC-2; center, **2** bound to KPC-2; right, **1** bound to KPC-2. Hydrogen bonds are depicted as dashed lines; the distances for key hydrogen bonds are shown (in Å). The deacylation water molecule is labeled as W#1. The two conformations for the sulfate moiety in **3** are labeled similarly to those in panel A.

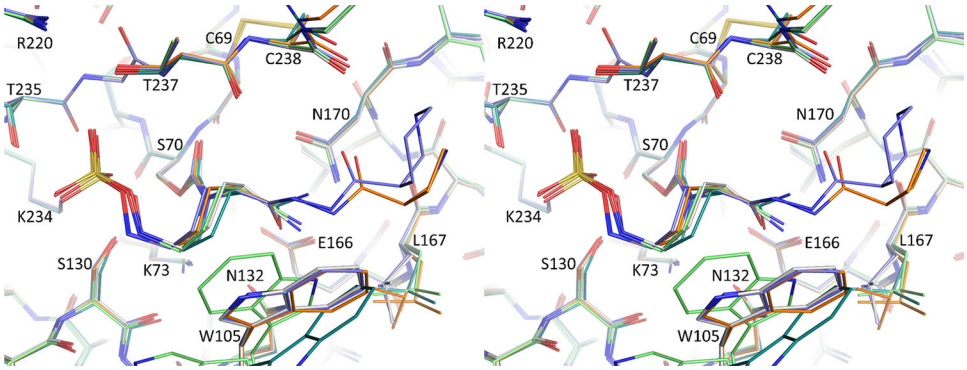

Figure 5.

Stereo figure of superimpositioning of DBO inhibitors in the active site of KPC-2. Depicted are **3** bound to KPC-2 molecule A (gray), **3** bound to KPC-2 molecule B (light green), **2** bound to KPC-2 molecule A (blue), **1** bound to KPC-2 molecule A (gold), avibactam bound to KPC-2 molecule A (dark green; PDB ID: 4ZBE). Structures used for the superimposition are from inhibitor-soaked KPC-2 crystals.

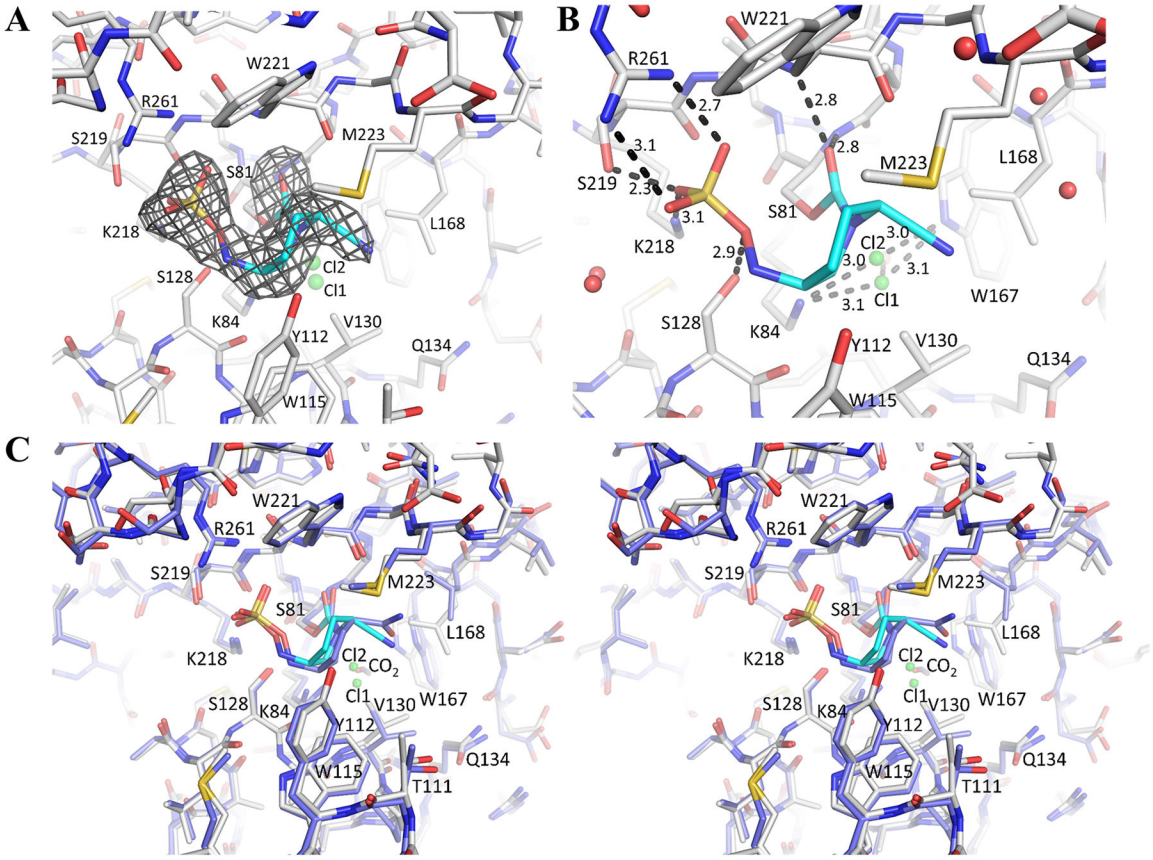

Figure 6.

Compound **3** bound to OXA-24. (A) Unbiased omit $|F_o|$-$|F_c|$ electron density of **3**:OXA-24 complex with the ligand removed from refinement and map calculations. Density is contoured at the 3σ level. (B) Interactions of **3** in the active site of OXA-24; the distances for key hydrogen bonds are shown (in Å). (C) Stereo figure depicting the superimpositioning of OXA-24 in complex with **3** (cyan **3** carbon atoms and gray protein carbon atoms) and in complex with avibactam (blue carbon atoms for avibactam and protein; PDB ID: 4WM9). In close proximity to the **3** ligand, a chloride ion in two alternate positions is present and labeled Cl1 and Cl2.

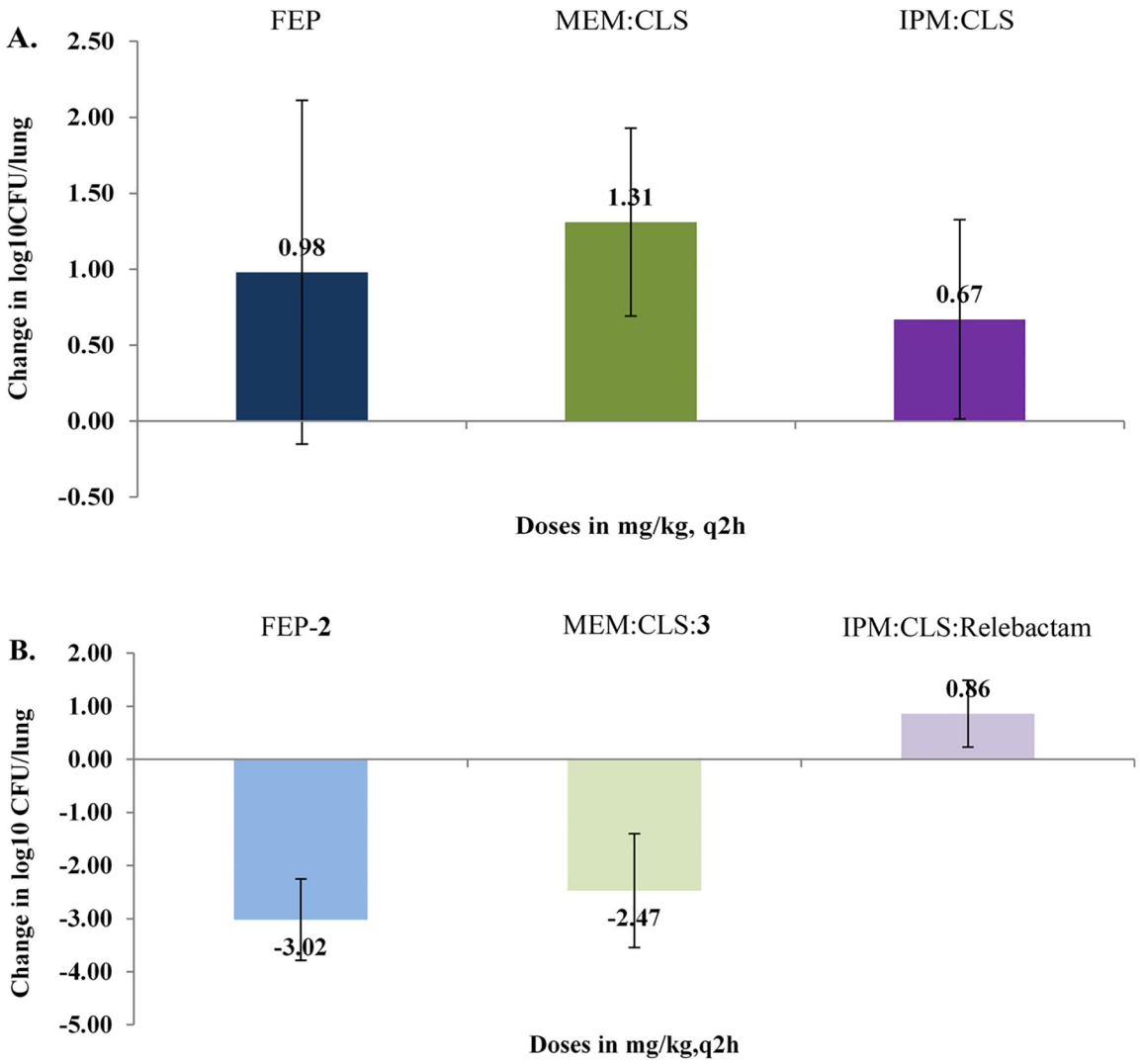

Figure 7.

A murine neutropenic lung infection model using a clinical isolate of *A. baumannii* SL06 carrying bla_{OXA-23} and bla_{OXA-51}. The graphs represent the change in CFU/lung after different antibiotic treatments were administered as q2h. (A) Cefepime at 50 mg/kg (FEP), meropenem:cilastatin at a 1:1 ratio of 25 mg/kg (MEM:CLS), and imipenem:cilastatin at a 1:1 ratio of 25 mg/kg (IPM:CLS). (B) Cefepime-**2** at 50 mg/kg and 8.33 mg/kg, respectively (FEP-**2**), meropenem:cilastatin at a 1:1 ratio of 25 mg/kg and 4.68 mg/kg of **3** (MEM:CLS-**3**), and imipenem:cilastatin at a 1:1 ratio of 25 and 18.75 mg/kg of relebactam (IPM:CLS-REL), respectively.

Table 1.

Kinetic Parameters

KPC-2	Ki app (μM)	k2/K (M−1 s−1)	koff (s−1)	half-life (min)	Kd (nM)	kcat/kinact
3	0.32 ± 0.03	$2.4 \pm 0.9 \times 10^5$	$4.5 \pm 0.5 \times 10^{-4}$	26 ± 3	1.9 ± 0.2	1
2	4.5 ± 0.5	$9.4 \pm 0.6 \times 10^3$	$4.0 \pm 0.4 \times 10^{-4}$	29 ± 3	43 ± 5	1
1	7.8 ± 0.8	$8.8 \pm 0.9 \times 10^3$	$3.5 \pm 0.5 \times 10^{-4}$	33 ± 5	40 ± 7	1
avibactam	0.9 ± 0.1	1.3×10^4[a]	1.4×10^{-4}[a]	$_{82}$[a]	11[a]	1
relebactam	2.2 ± 0.3	$2.8 \pm 0.3 \times 10^4$	$2.5 \pm 0.5 \times 10^{-4}$	46 ± 9	9 ± 2	1
ADC-7	$K_{i\ app}$ (μM)	k_2/K (M^{-1} s^{-1})	k_{off} (s^{-1})	half-life (min)	K_d (nM)	k_{cat}/k_{inact}
3	8.0 ± 0.8	$1.9 \pm 0.2 \times 10^4$	$1.0 \pm 0.1 \times 10^{-3}$	12 ± 2	53 ± 7	6
2	2.3 ± 0.3	$3.5 \pm 0.4 \times 10^4$	$1.1 \pm 0.1 \times 10^{-3}$	11 ± 1	32 ± 3	4
1	3.7 ± 0.4	$3.2 \pm 0.3 \times 10^4$	$9.0 \pm 0.1 \times 10^{-4}$	13 ± 1	29 ± 3	4
avibactam	19 ± 2	$3.9 \pm 0.4 \times 10^3$	$3.5 \pm 0.5 \times 10^{-4}$	33 ± 5	90 ± 9	4
relebactam	12.6 ± 2	$7.8 \pm 0.8 \times 10^3$	$3.0 \pm 0.3 \times 10^{-4}$	39 ± 4	39 ± 4	2
PDC-3	$K_{i\ app}$ (μM)	k_2/K (M^{-1} s^{-1})	k_{off} (s^{-1})	half-life (min)	K_d (nM)	k_{cat}/k_{inact}
3	3.8 ± 0.4	$2.3 \pm 0.2 \times 10^4$	$2.8 \pm 0.3 \times 10^{-3}$	4.1 ± 0.4	124 ± 18	5
2	0.14 ± 0.01	$4.8 \pm 0.7 \times 10^5$	$3.5 \pm 0.4 \times 10^{-3}$	3.3 ± 0.4	7.3 ± 1.4	1
1	0.13 ± 0.02	$6.3 \pm 0.6 \times 10^5$	$4.0 \pm 0.4 \times 10^{-3}$	2.9 ± 0.3	6.3 ± 0.9	1
avibactam	2.5 ± 0.3[a]	2.9×10^4[a]	8×10^{-4}[a]	14.4[a]	27.6[a]	1
relebactam	3.2 ± 0.3	$4.6 \pm 0.5 \times 10^4$	$9.0 \pm 0.1 \times 10^{-4}$	12.8 ± 1.4	20 ± 3	1
OXA-23	$K_{i\ app}$ (μM)	k_2/K (M^{-1} s^{-1})	k_{off} (s^{-1})	half-life (min)	K_d (nM)	k_{cat}/k_{inact}
3	8±1	$1.7 \pm 0.2 \times 10^4$	$5.0 \pm 0.5 \times 10^{-4}$	23 ± 2	29 ± 4	1
2	>100	ND	ND	ND	ND	ND
1	>100	ND	ND	ND	ND	ND
avibactam	>100	3×10^2[a]	8.0×10^{-6}[a]	1,436[a]	$_{27}$[a]	ND
relebactam	>100	ND	ND	ND	ND	ND
OXA-24/40	$K_{i\ app}$ (μM)	k_2/K (M^{-1} s^{-1})	k_{off} (s^{-1})	half-life (min)	K_d (nM)	k_{cat}/k_{inact}
3	5.0 ± 0.5	$9.6 \pm 1.0 \times 10^3$	$4.0 \pm 0.4 \times 10^{-4}$	29 ± 3	42 ± 6	2
2	>100	ND	ND	ND	ND	ND
1	>100	ND	ND	ND	ND	ND
avibactam	>100	5.2×10^1[a]	6.3×10^{-6}[a]	1,823[a]	121[a]	ND
relebactam	>100	ND	ND	ND	ND	ND
OXA-48	$K_{i\ app}$ (μM)	k_2/K (M^{-1} s^{-1})	k_{off} (s^{-1})	half-life (min)	K_d (nM)	k_{cat}/k_{inact}
3	0.29 ± 0.03	$6.4 \pm 0.6 \times 10^5$	$9.0 \pm 0.1 \times 10^{-4}$	13 ± 1	1.4 ± 0.2	2
2	>100	ND	ND	ND	ND	ND
1	>100	ND	ND	ND	ND	ND
avibactam	30 ± 3	1.4×10^3[a]	$1.2 \pm \times 10^{-5}$[a]	1,000[a]	$_{9}$a	1
relebactam	>100	ND	ND	ND	ND	ND

[a]Previously published data.[4,5] ND: if $K_{i\ app}$ values were >100 μM, then further kinetic analyses were not determined.

Table 2.

Mass Spectrometry Data for β-Lactamases Incubated with DBOs for 5 min and 24 h

		5 min		24 h	
sample	**inhibitor**	**molecular weight (M_W)**	**ΔM_W(ΔDBO)**	**M_W**	**ΔM_W (ΔDBO)**
KPC-2	none	28,723	+0	28,724	+0
KPC-2	3	28,971	+247	28,971	+247
KPC-2	2	29,115	+392	29,115	+392
KPC-2	1	29,101	+378	29,101	+378
KPC-2	avibactam	28,989	+266	28,989	+265
				28,892	+168 (−97)
KPC-2	relebactam	29,071	+349	29,072	+350
ADC-7	none	40,639	+0	40,640	+0
ADC-7	3	40,639 (minor)	+0	40,640	+0
		40,886	+248	40,887	+247
		40,806 (minor)	+166 (−80)	40,806 (minor)	+166 (−80)
ADC-7	2	40,639 (minor)	+0	40,640	+0
		41,030	+391	41,031 (minor)	+247
ADC-7	1	40,639	+0	40,640	+0
		41,016	+377	41,018 (minor)	+377
ADC-7	avibactam	40,640 (minor)	+0	40,641	+0
		40,904	+264	40,905	+264
		40,824 (minor)	+185 (−80)	40,824	+185 (−80)
ADC-7	relebactam	40,639 (minor)	+0	40,989	+348
		40,987	+349		
PDC-3	none	40,654	+0	40,655	+0
		40,785	+0	40,786	+0
PDC-3	3	41,033	+246	41,033	+246
		40,902	+246	40,903	+246
		40,951 (minor)	+166 (−80)	40,951 (minor)	+166 (−80)
		40,820 (minor)	+166 (−80)	40,822 (minor)	+166 (−80)
PDC-3	2	41,177	+394	41,178	+394
		41,046	+394	41,046	+394
PDC-3	1	41,163	+383	41,163	+383
		41,032	+383	41,032	+383
PDC-3	avibactam	41,051	+265	41,051	+265
		40,920	+265	40,920	+265
		40,970 (minor)	+185 (−80)	40,970 (minor)	+185 (−80)
		40,840 (minor)	+185 (−80)	40,840 (minor)	+185 (−80)
PDC-3	relebactam	41,134	+353	41,134	+353
		41,003	+353	41,004	+353
OXA-23	none	27,494	+0	27,494	+0
OXA-23	3	27,494 (minor)	+0	27,494 (minor)	+0

		5 min		24 h	
sample	**inhibitor**	**molecular weight (M_W)**	**ΔM_W(ΔDBO)**	**M_W**	**ΔM_W (ΔDBO)**
		27,740	+246	27,741	+247
		27,660 (minor)	+166 (−80)	27,660 (minor)	+167 (−80)
OXA-24/40	none	28,664	+0	28,664	+0
OXA-24/40	3	28,664 (minor)	+0	28,665 (minor)	+0
		28,911	+247	28,912	+247
		288,32 (minor)	+166 (−80)	28,832 (minor)	+166 (−80)
OXA-48	none	28,283	+0	28,290	+0
OXA-48	3	28,283 (minor)	+0	28,286 (minor)	+0
		28,530	+247	28,533	+247
		28,449 (minor)	+166 (−80)	28,451 (minor)	+166 (−80)
OXA-48	avibactam	28,549	+266	28,551	+265
		28,468 (minor)	+185 (−80)		

cefepime/avibactam-4	cefepime/relebactam-4	mero-penem	mero-penem/3–4	mero-penem/3–8	mero-penem/1–4	mero-penem/1–8	mero-penem/2–4	mero-penem/2–8	mero-penem/avibactam-4	mero-penem/ relebactam-4
Isogenic Strains										
<0.12	<0.12	<0.12	<0.12	<0.12	<0.12	<0.12	<0.12	<0.12	<0.12	<0.12
<0.12	<0.12	8	<0.12	<0.12	<0.12	<0.12	<0.12	<0.12	<0.12	<0.12
<0.12	<0.12	<0.12	<0.12	<0.12	<0.12	<0.12	<0.12	<0.12	<0.12	<0.12
<0.12	<0.12	0.5	<0.12	<0.12	<0.12	<0.12	<0.12	<0.12	<0.12	<0.12
<0.12	<0.12	<0.12	<0.12	<0.12	<0.12	<0.12	<0.12	<0.12	<0.12	<0.12
<0.12	<0.12	0.25	<0.12	<0.12	<0.12	<0.12	<0.12	<0.12	<0.12	0.25
0.5	0.25	<0.12	<0.12	<0.12	<0.12	<0.12	<0.12	<0.12	<0.12	<0.12
>16	>16	>16	16	4	>16	>16	>16	>16	>16	>16
roducing bla_{KPC}: Colis in Resistant (ColR) and Colis tin Susceptibile (ColS)										
<0.12	0.25	2	<0.12	<0.12	<0.12	<0.12	<0.12	<0.12	<0.12	<0.12
0.25	0.5	>16	<0.12	<0.12	<0.12	<0.12	<0.12	<0.12	<0.12	<0.12
0.5	1	>16	0.5	0.25	0.25	<0.12	<0.12	<0.12	<0.12	0.5
<0.12	<0.12	16	<0.12	<0.12	<0.12	<0.12	<0.12	<0.12	<0.12	<0.12
<0.12	<0.12	>16	<0.12	<0.12	<0.12	<0.12	<0.12	<0.12	<0.12	<0.12
<0.12	0.25	>16	<0.12	<0.12	<0.12	<0.12	<0.12	<0.12	<0.12	<0.12

cefepime/avibactam-4	cefepime/relebactam-4	mero-penem	mero-penem/3–4	mero-penem/3–8	mero-penem/1–4	mero-penem/1–8	mero-penem/2–4	mero-penem/2–8	mero-penem/avibactam-4	mero-penem/ relebactam-4
<0.12	0.25	16	<0.12	<0.12	<0.12	<0.12	<0.12	<0.12	<0.12	<0.12
<0.12	0.5	>16	<0.12	<0.12	<0.12	<0.12	<0.12	<0.12	<0.12	<0.12
<0.12	0.25	>16	<0.12	<0.12	<0.12	<0.12	<0.12	<0.12	<0.12	<0.12
<0.12	<0.12	16	<0.12	<0.12	<0.12	<0.12	<0.12	<0.12	<0.12	<0.12
<0.12	<0.12	16	<0.12	<0.12	<0.12	<0.12	<0.12	<0.12	<0.12	<0.12
roducing bla_{KPC}: Colistin Resistant (ColR) and Colistin Susceptibile (ColS)										
<0.12	0.25	8	<0.12	<0.12	<0.12	<0.12	<0.12	<0.12	<0.12	<0.12
<0.12	<0.12	16	<0.12	<0.12	<0.12	<0.12	<0.12	<0.12	<0.12	<0.12
<0.12	1	>16	<0.12	<0.12	<0.12	<0.12	<0.12	<0.12	<0.12	<0.12
erobacteriaceae Isolates Producing $bla_{OXA\text{-}48}$ and mutants										
0.25	2	>16	<0.12	<0.12	1	<0.12	<0.12	<0.12	1	>16
0.5	4	>16	<0.12	<0.12	<0.12	<0.12	1	<0.12	1	16
0.25	2	8	<0.12	<0.12	<0.12	<0.12	<0.12	<0.12	<0.12	8
0.5	2	>16	0.25	<0.12	<0.12	<0.12	<0.12	<0.12	0.5	>16
1	4	>16	0.25	0.25	0.5	0.5	1	<0.12	1	16
<0.12	0.25	2	<0.12	<0.12	<0.12	<0.12	<0.12	<0.12	<0.12	2
-Avibactam-Resistant Clinical *P. aeruginosa* Isolates[28]										

cefepime/avibactam-4	cefepime/relebactam-4	mero-penem	mero-penem/3–4	mero-penem/3–8	mero-penem/1–4	mero-penem/1–8	mero-penem/2–4	mero-penem/2–8	mero-penem/avibactam-4	mero-penem/ relebactam-4
>16	16	>16	>16	>16	>16	16	>16	>16	>16	>16
16	16	>16	>16	16	16	0.5	16	8	16	16
>16	16	>16	16	>16	16	16	16	16	>16	>16
>16	>16	16	16	16	4	<0.12	16	4	16	8
4	4	1	1	1	<0.12	<0.12	0.5	<0.12	1	1
aumannii Isolates Producing *bla*$_{\mathbf{OXA}\text{-}23}$ and/or bla$_{\mathbf{OXA}\text{-}24}$										
>16	>16	>16	>16	>16	>16	>16	>16	>16	>16	>16
>16	>16	>16	16	16	>16	>16	>16	>16	>16	>16
16	16	>16	4	4	>16	>16	>16	>16	>16	>16
>16	16	>16	4	2	>16	>16	>16	>16	>16	>16
>16	>16	>16	>16	>16	>16	>16	>16	>16	>16	>16
>16	16	>16	>16	>16	>16	>16	>16	>16	>16	>16
aumannii Isolates Producing *bla*$_{\mathbf{OXA}\text{-}23}$ and/or bla$_{\mathbf{OXA}\text{-}24}$										
>16	>16	>16	16	8	>16	>16	>16	>16	>16	>16
16	>16	>16	4	**2**	>16	>16	>16	>16	>16	>16
16	16	>16	**2**	1	>16	>16	>16	>16	>16	>16
>16	>16	>16	>16	16	>16	>16	>16	>16	>16	>16
2	**2**	0.25	0.25	0.25	0.25	0.25	0.25	0.25	0.25	0.25
>16	>16	>16	>16	>16	>16	>16	>16	>16	>16	>16

Table 4.

In Vivo Efficacy of Cefepime-2, Meropenem-3, and Comparators in the Peritonitis Model

strains	β-lactamases	infecting load CFU/mouse	treatment protocol[a]	antibiotics	MIC (μg/mL)[b]	PD_{50} (mg/kg)	PD_{90} (mg/kg)
A. *baumannii* NCTC 13301	OXA-23, OXA-51	3.5×10^5	+1 h PI, 2 doses	cefepime	>256	>100	>100
				cefepime-2[c]	16	100 + 23.23	100 + 52.30
		3.5×10^6	+1 h PI, 2 doses	meropenem[d]	32	>100	>100
				meropenem-3	1	25 + 16.30	25 + 23.71
				tigecycline	1	>6.25	>6.25
			3 doses	colistin	1	16.57	NA
A. *baumannii* NCTC 13303	OXA-26, OXA-51- like	2.5×10^6	+1 h PI, 2 doses	cefepime	64	>200	>200
				cefepime-2	16	50 + <23.23	50 + 23.23
			+2 h PI, 2 doses	meropenem	256	>100	>100
				meropenem-3	16	50 + 24.01	50 + 49.38
				tigecycline	1	>6.25	>6.25
			3 doses	colistin	0.5	11.72	18.72
A. *baumannii* SL46	OXA-23, OXA-51	3×10^6	+1 h PI, 2 doses	cefepime	>512	>200	>200
				cefepime-2	32	50 + 23.23	100 + 52.30
			+2 h PI, 2 doses	meropenem	64	>100	>100
				meropenem-3	8	50 + 24.91	50 + 66.17

[a] Abbreviations: PI, postinfection; 2 doses, the drugs were administered twice, 3 h apart; 3 doses, the drugs were administered thrice, 3 h apart.

[b] For MIC determinations, **3** was used at a fixed 8 μg/mL concentration. Cefepime-**2** MICs were determined at 1:1 ratio.

[c] Compound **2** as a monotherapy at 200 mg/kg did not result in protection of infected animals.

[d] Meropenem was administered in combination with cilastatin (1:1) due to meropenem's instability to murine renal DHP-1.[50]